ANL-6124
Reactors - General
(TID-4500, 15th Ed.)
AEC Research and
Development Report

ARGONNE NATIONAL LABORATORY
9700 South Cass Avenue
Argonne, Illinois

THE INTERNAL FEEDBACK OF EBR-I MARK-III

by

J. C. Carter

Reactor Engineering Division

and

D. W. Sparks and J. H. Tessier
Land-Air, Inc.

February 1960

Operated by The University of Chicago
under
Contract W-31-109-eng-38

DISCLAIMER

DISTRIBUTION OF WORK

REACTOR	MODEL
F. W. Thalgott	D. Okrent
J. F. Boland	J. C. Carter
J. K. Long	D. W. Sparks
R. E. Rice	J. H. Tessier
R. R. Smith	

CONTRIBUTIONS AND SUGGESTIONS

R. O. Brittan
H. Greenspan
H. H. Hummel
H. A. Sandmeier
J. A. Thie
E. T. Wakler
J. H. Wheeler

TABLE OF CONTENTS

LIST OF FIGURES

LIST OF FIGURES

THE INTERNAL FEEDBACK OF EBR-I MARK-III

J. C. Carter,* D. W. Sparks** and J. H. Tessier**

ABSTRACT

The reactor is considered to constitute a closed-loop, nonlinear mechanical system with forcing functions resulting from variations in neutron density and the flow of NaK. The significant sources of internal feedback are found to be the variation in volume of the uranium and the variation in the density of NaK. Resistance to the free motion of uranium in response to thermal expansion accounts for the significant nonlinear properties of the system. This resistance results from the physical characteristics of the redundant structure constituting the core, blankets and containing shell.

The mechanical system has been transformed into a dynamically similar electronic system which is subject to the transformed operating conditions of the reactor.

All the equations defining the time-dependent physical phenomena were developed from an analysis of the mechanical system. Only the constants in the nonlinear equations of motion of the materials of the core and blankets were synthesized from low-power operation of the reactor.

The relationship between signal and response of the two systems is in good agreement over all conditions of operation.

NOMENCLATURE

A	cross-sectional area
a	width; also see eq. (19)
b	see eq. (19)
C_f	constant of proportionality
C	concentration of neutron precursors
c	viscous damping coefficient
c_c	critical viscous damping coefficient
c_p	specific heat

*Argonne National Laboratory

**Land-Air, Inc.

NOMENCLATURE

D_h	vertical displacement
E	modulus of elasticity
F	kinetic friction force
F_c	constant normal force
F_r	static friction force
f	frequency
G	closed loop describing function
G_0	neutron kinetics transfer function
$G(v_c)$	a function of velocity
g	acceleration of gravity
H	feedback describing function; heat transferred
h	heat transfer rate coefficient
k	thermal conductivity; reactivity; spring constant
k_{ex}	excess reactivity
ℓ	neutron lifetime; length
M	reactive couple
m	mass
N	total normal force
n	neutron density
P	pressure; power
Q	total heat
q	heat per unit volume
R	radius of a region
r	radius of a rod
S	surface for heat transfer
s	Laplacian operator
T	temperature; time
t	time
V	strain energy
v_c	coolant velocity

NOMENCLATURE

X	restrained motion of equivalent mass m
X_f	$\Delta\ell$ free motion of equivalent mass m
x	$\frac{X}{\ell}$ unit restrained motion
x_f	$\frac{X}{\ell}$ f unit free motion assumed equal to $\frac{\Delta\ell}{\ell}$
Z	length of a rod
α	coefficient of expansion; μ_0/μ
β	fraction of total fission neutrons which are delayed
δ	Δr concomitant with V; relative jump
ϵ	an arbitrary velocity
λ	decay constant
ζ	damping ratio
μ	kinetic friction coefficient
μ_0	static friction coefficient
ρ	density
σ	stress (plane)
ν	Poisson ratio
Φ , ϕ	phase angle
τ	stress (shear); time constant; transport lag
ω	frequency

Subscripts

c	NaK coolant
r	radial
t	tangential
u	uranium
z	zirconium
0	reference point
1	inlet
2	outlet

INTRODUCTION

This is a presentation of the results of an investigation of the dynamic characteristics of EBR-I Mark-III (Fig. 1). The core and concentric blanket of this reactor consist of a vertical bundle of zirconium-clad uranium rods in a concentric cylindrical steel shell. The rods are separated from each other and from the steel shell by radial spacers, thus permitting NaK to flow through the bundle parallel to the longitudinal axis of the core. The core is 22 cm in diameter and 21 cm high. The outside diameter of the radial blanket is 39 cm. There are top and bottom blankets. The blanket consists of twelve hexagonal groups of 36 depleted uranium rods. There is no moderator.

The diameter of each uranium rod is 0.925 cm. All zirconium cladding is 0.050 cm thick. Each zirconium spacer is 0.117 cm in diameter.

The flow through the blanket may be in series or in parallel during any test. The NaK inlet temperature and velocity through the tube bundle may be varied at will.

During steady-state operation the heat generated by fission of the uranium is just balanced by the heat carried away by the NaK, and the reactivity is constant. Any induced change in reactivity upsets the balance. An unbalance in thermodynamic conditions will in turn affect the nuclear characteristics and modify the effect of the change in reactivity. It is this inherent modifying effect of the reactor that is of concern. It is a unique feature of each design and one that is controlled by the reactor designer. A successful reactor will respond satisfactorily to the signals which it receives in the service to which it is applied.

Dynamically, the reactor is considered to represent a closed-loop, nonlinear mechanical system with many degrees of freedom. This system is subject to forced vibrations which are damped by the resistance to motion of the components of the system. The forcing functions result from variations in neutron density and the flow of NaK. These variations in turn are produced by arbitrarily induced variations in reactivity in the form of sinusoidal waves, ramps, or steps, and in the NaK flow by changing velocities and inlet temperature. The damping is manifest by resistance to the free response of the system to these signals. It is the restrained movement of the uranium which provides the significant nonlinearities in the response of the reactor. This damping is determined from an analysis of the structural arrangement and physical properties of the core and blanket. It is evidenced to varying degrees by friction between components which move relative to each other, by bowing, by elastic buckling, by warping, and by elastic and plastic deformation.

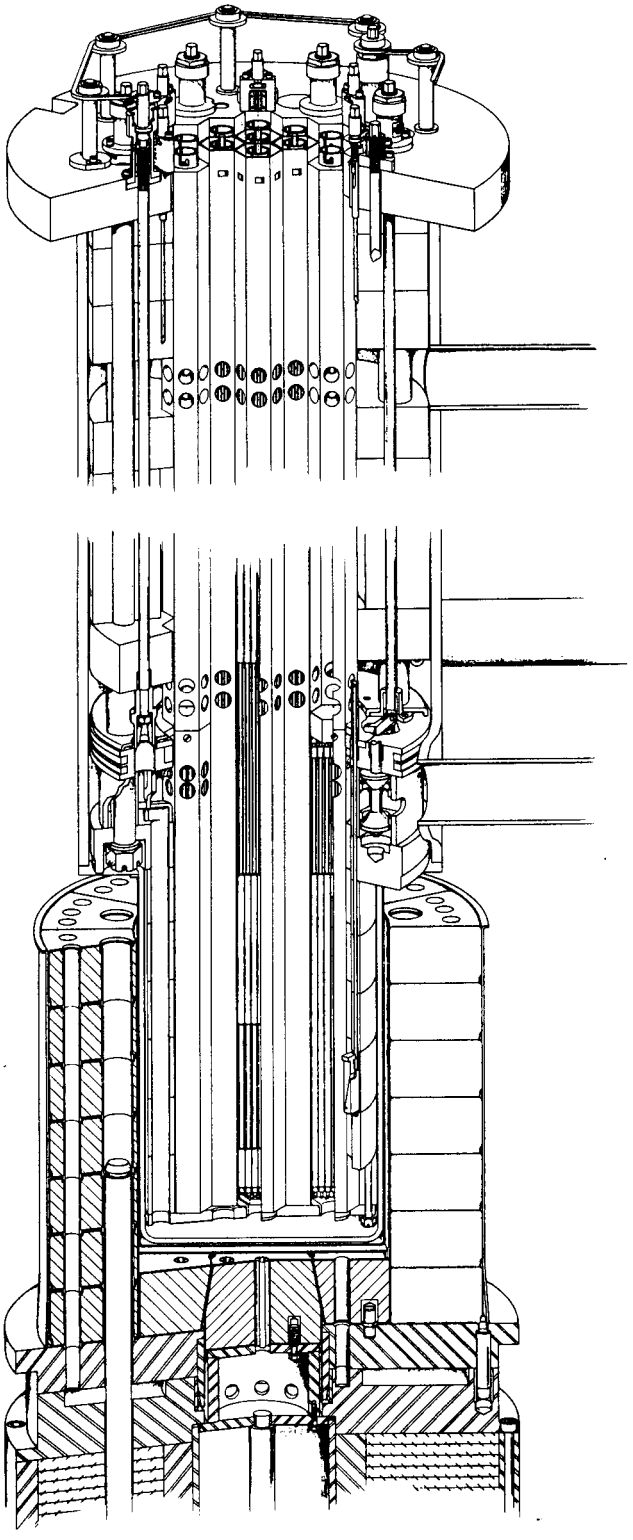

Fig. 1

Cross Section of EBR-I Mark III

Since reactor cores are complex nonlinear systems, the relationship between cause and effect is a function of a large number of interrelated variables. These variables are associated with the interaction of the nuclear, thermodynamic, fluid dynamic, and mechanical phenomena of the core. They may be dependent upon energy, space, and time. Exact equations defining the dynamic behavior of a specific reactor are extremely complex and have not been written. A few relatively simple equations will have to suffice for the present. It is expected that it will be possible eventually to write with confidence the equations which will define adequately the dynamic performance of a proposed design. Currently, every analytically determined feedback should be substantiated by implicit synthesis.*

The effective reactivity at steady state is unity. If for any reason there is an excess of reactivity from external sources or from self-induction, then the physical phenomena of the reactor are in a transitory state, but if there is an inherent stabilizing effect, such as a negative feedback, the reactor will return to steady-state operation, most likely at a different power level. The anticipated sources of internal feedback were considered and their effects upon reactivity were evaluated by static calculations. Some of the sources of feedback are found in the effect of poisons, built-in reactivity, moderator, coolant dynamics, variable voids, and temperature. Short-term effects are predominantly a function of temperature.

Variations in temperature throughout the reactor cause dimensions, densities, and the Doppler effect to vary. These variations cause reactivity to vary and, since the reactor is a closed-loop system, to modify any perturbation of the steady state.

In this particular reactor, the only significant sources of feedback were found to be the change in the number of atoms of U and NaK per unit volume of core and blanket. This was expressed in the following manner:

$$\Delta k = \begin{cases} \text{Core} & \text{Radial blanket} \\ 0.31 \ \Delta\ell/\ell & 0.1 \ \Delta\ell/\ell \\ 0.62 \ \Delta R/R & 0.2 \ \Delta R/R \\ 0.005 \ \Delta\rho/\rho & 0.02 \ \Delta\rho/\rho \end{cases}$$

*A. B. Clymer, Direct System Synthesis by Means of Computers. AIEE Transactions, Paper No. 58-1003. Paper presented Aug. 19, 1958. Implicit synthesis is a valuable analog computing technique which uses actual responses to determine unknown variables. Fortuitous features of the kinetics equations make the technique particularly applicable to determining the feedback reactivity of a reactor.

The unit expansion of the diameter of individual rods, $\Delta r/r$, affects reactivity indirectly, because it creates the variable force which is superimposed on the initial mechanical clamping of the core and blanket fuel.

The constants relating the change in metal volume and NaK density to reactivity were determined initially from the application of diffusion theory to static conditions and were substantiated by the synthesis of low-power operating data.

The quantities $\Delta\ell/\ell$, $\Delta R/R$, $\Delta r/r$ and $\Delta\rho/\rho$ are determined as functions of the transient metal temperatures. Their determinations are unique to each reactor. The mathematical equations of the phenomen in which these sources of feedback occur define the generalized feedback mechanism for any condition of operation or signal.

The time dependence associated with the feedback $\Delta\rho/\rho$, pertaining to the density of NaK, is implicit in the equations of thermodynamics. Variations in NaK density are simple direct feedbacks.

The magnitudes and time constants associated with unrestrained variations in $\Delta\ell/\ell$, $\Delta R/R$, and $\Delta r/r$ depend upon the thermodynamic characteristics of the reactor.

This investigation is concerned with how Mark III responds to the forcing functions.

A simple block diagram is presented in Fig. 2 to illustrate the concept of the closed-loop system represented by the reactor and to define terms used throughout.

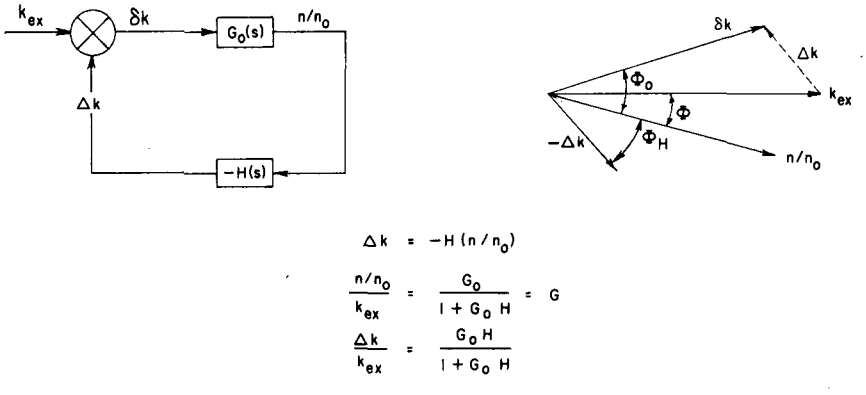

$$\Delta k = -H(n/n_o)$$

$$\frac{n/n_o}{k_{ex}} = \frac{G_o}{1 + G_o H} = G$$

$$\frac{\Delta k}{k_{ex}} = \frac{G_o H}{1 + G_o H}$$

Fig. 2. A Closed-Loop Diagram of a Reactor

The responses of the reactor to the forcing functions show that it is a closed-loop system with nonlinear feedback. The nonlinear characteristics of the reactor are discussed in the section titled "Nonlinear Characteristics of the Reactor."

DESCRIPTION OF THE MODEL

It was necessary to represent a complex nonlinear mechanical system by an equivalent electronic system. The block diagram whereby this was done is shown on Fig. 3a and the analog diagram on Fig. 3b. The only semblance between the two systems is that they are dynamically similar and respond in the same manner to any given signal.

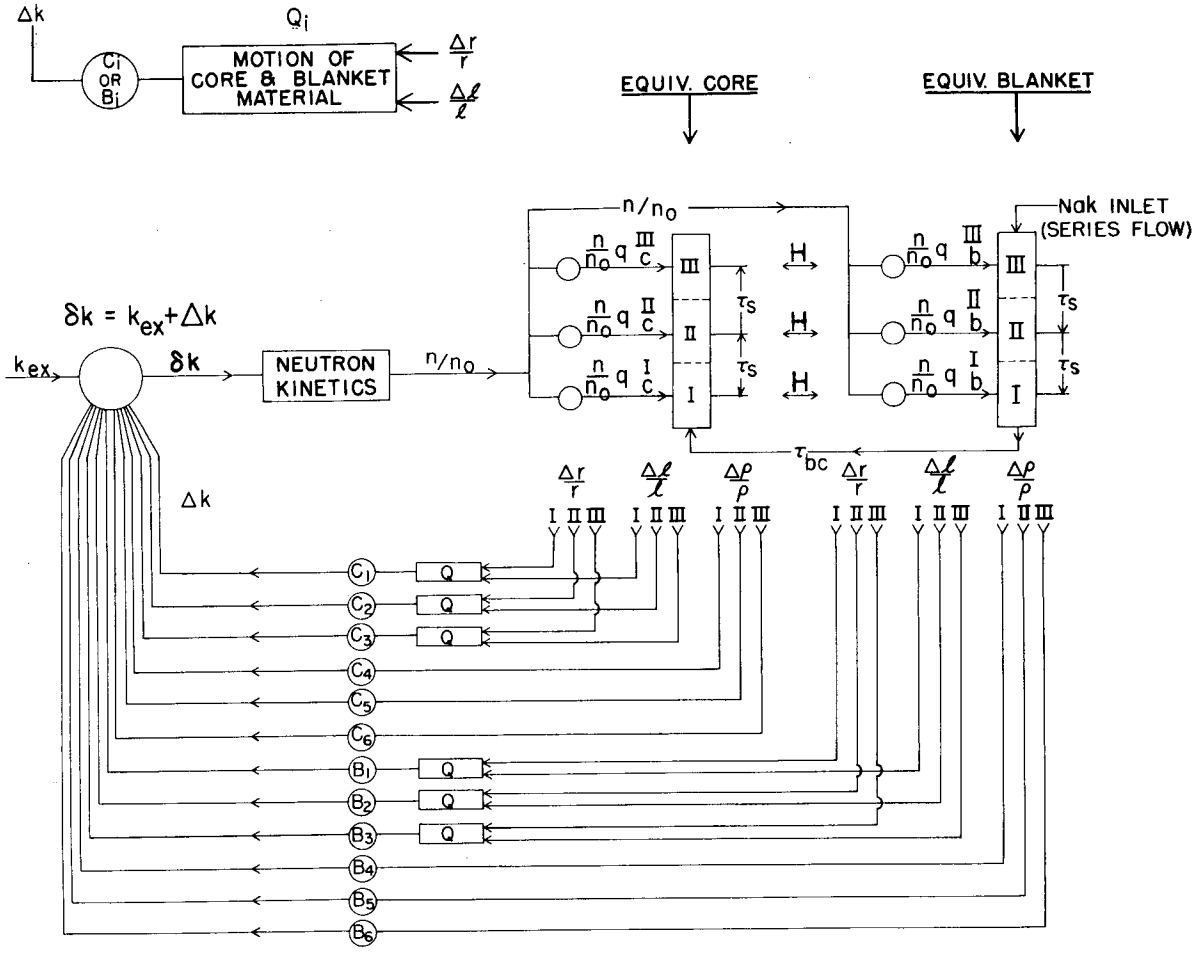

Fig. 3a. Block Diagram of the Model for EBR-I, Mark III

The electronic analogs of the core and blankets are represented schematically in Fig. 3a by two rods. These dynamically equivalent representations were (figuratively) sectionalized radially and axially (Fig. 4), and the average condition in core and blanket was expressed in terms of single rods. The equivalent heat generation and worth of each were determined and the movements of the rods and the variations of NaK density were expressed in terms of reactivity $\Delta k/k$. The determination

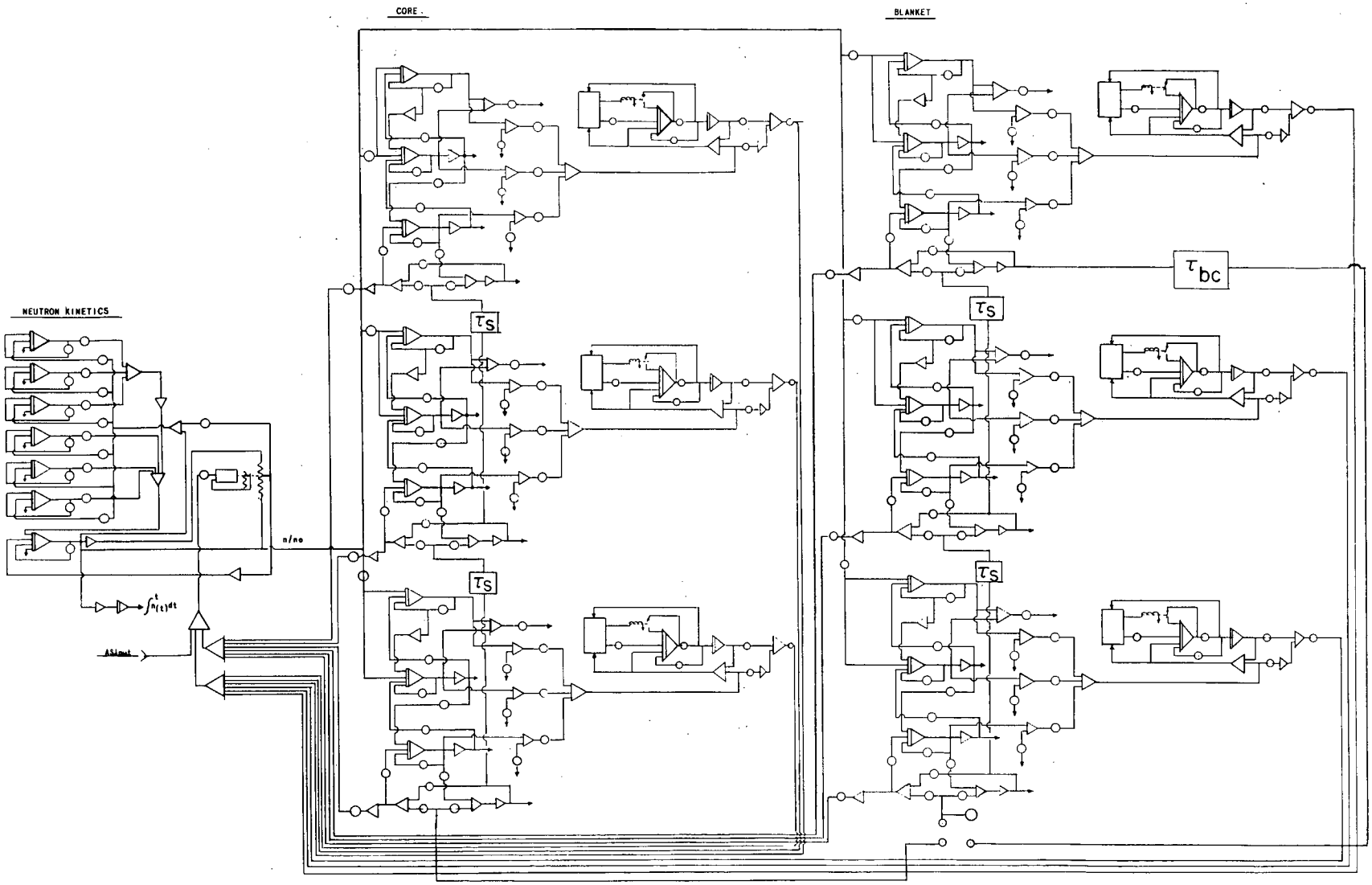

Fig. 3b. The Analog Diagram of the Model

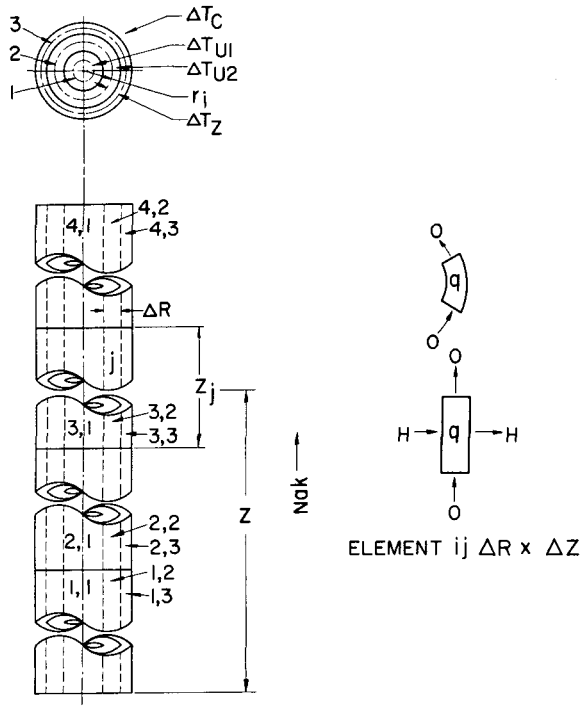

Fig. 4. Volumetric Division of a Rod of EBR-I, Mark III

of the power distribution, the reactivity worths of various areas of the core, and the relationship of reactivity to various reactivity-producing parameters were based on an unpublished work.*

All phenomena were considered in terms of the actual physical characteristics of the reactor and then converted to the dynamically equivalent circuitry of the electronic analog system.

If every rod were free to move as thermal forcing functions dictated, the reactor would represent essentially a linear system at any constant NaK velocity, quite easy to analyze by well-developed linear theory. However, the rods do not expand uniformly nor do they move freely. The gain and feedback due to thermal phenomena are not sufficient to define the nonlinear response. This feedback is modified by nonlinear mechanical effects which decrease the feedback gain and increase the feedback lag.

The volumetric changes are represented by

$$\left(\frac{\Delta \ell}{\ell} + \frac{2\,\Delta R}{R}\right) = \frac{3\,\Delta \ell}{\ell}$$

and the NaK density changes by $\Delta\rho/\rho$. If there were no restraints to free expansion, both $\Delta\ell/\ell$ and $\Delta\rho/\rho$ would be converted to reactivity and feed back into the input. There are restraints to free expansion, so $\Delta\ell/\ell$ is fed into Block Q (Fig. 3a) and comes out decreased in magnitude and increased in phase angle. It is then converted to Δk and combined with the input signal.

*A. Fenstermacher, Power coefficient calculations for EBR-I, Mark III, by Argonne National Laboratory (November 11, 1957).

EQUATIONS

All of the equations defining the concomitant physical phenomena which significantly affect internal feedback in the reactor during the period of perturbation were derived from analysis of the physical characteristics of the core and blankets. The equations which describe the phenomena fall into four categories:

(a) Neutron Kinetics
(b) Thermodynamics
(c) Elasticity
(d) Nonlinear Mechanics

(a) Neutron Kinetics

$$\frac{dn}{dt} = \frac{-\beta n + k_{ex}(1-\beta)n}{\ell} + \sum_{i=1}^{6} \lambda_i C_i \qquad (1)$$

$$\frac{dC_i}{dt} = \frac{\beta_i n + k_{ex}\beta_i n}{\ell} - \lambda_i C_i \quad ; \quad i = 1 \longrightarrow 6 \qquad (2)$$

$\ell = 1 \times 10^{-7}$ sec .

Keepin Constants

i	$\beta_i (\times 10^3)$	λ_i, sec^{-1}
1	0.228	3.8700
2	0.974	1.4000
3	2.760	0.3110
4	1.257	0.1153
5	1.377	0.0318
6	0.234	0.0127

(b) Thermodynamics

Heat generated in the uranium by fission flows to the surface of the uranium by conduction. Heat is conducted through the non-heat generating zirconium and, at the outer surface, is transferred to the NaK by convection and conduction.

It is assumed that the curves of power vs. the distance along the longitudinal and radial axes do not change shape and that the level of power varies directly as the neutron density.

A continuous solution of the heat transfer equations gives a Δk which is a continuous function of velocity and of position along a fuel rod. The magnitude and phase angle increase in the direction of NaK flow because the transportation of NaK along the rod increases the heat level of the NaK downstream and, in turn, the temperature of the metal, but the effect is delayed by the transport time.

The basic equations of heat flow for this particular arrangement are considered to be as follows:

1. Radial temperature distribution in the uranium:

$$c_p \rho \frac{\partial T(r,t)}{\partial t} = k \left\{ \frac{\partial^2 T(r,t)}{\partial r^2} + \frac{1}{r} \frac{\partial T(r,t)}{\partial r} \right\} + \frac{n}{n_0} q(t) \quad . \tag{3}$$

Heat is assumed to be generated uniformly and no account is taken of the effect of axial flow of heat.

2. Radial temperature distribution in the zirconium cladding:

$$c_p \rho \frac{\partial T(r,t)}{\partial t} = k \left\{ \frac{\partial^2 T(r,t)}{\partial r^2} + \frac{1}{r} \frac{\partial T(r,t)}{\partial r} \right\} \quad . \tag{4}$$

3. Heat transferred from the surface of the zirconium cladding to NaK:

$$Q = h S \frac{\left(T_{z1} - T_{c1}\right) - \left(T_{z2} - T_{c2}\right)}{\ell n \left(\frac{T_{z1} - T_{c1}}{T_{z2} - T_{c2}} \right)} \quad . \tag{5}$$

It was not feasible under the circumstances to attempt a continuous solution of these fundamental equations of heat flow. It was necessary to resort to a step solution. The fuel rods were sectionalized into cylindrical shells of thickness ΔR and length ΔZ. The average conditions in each cylindrical element were summed over the volume of a rod (Fig. 4). The average temperature in an element $2\pi r_i \Delta Z_j$ was determined from the time-dependent heat balance in the element.

Heat storage = heat generation + heat entering - heat leaving.

The inlet NaK temperature to element ΔZ_i is the outlet NaK temperature from the element ΔZ_{i-1}. Log mean temperature differences were used between zirconium and NaK in computing the convective heat transfer. The convection heat transfer rate is a function of NaK velocity, the geometry of the flow channel, and the temperature of the materials involved in the heat transfer.

A rod was not assumed to be homogeneous but bimetallic, the zirconium being a nongenerating conductor and playing a significant part in the calculation of $\Delta\ell/\ell$ and $\Delta r/r$.

The dimensions and physical data pertaining to the solution of these equations are contained in Appendix A.

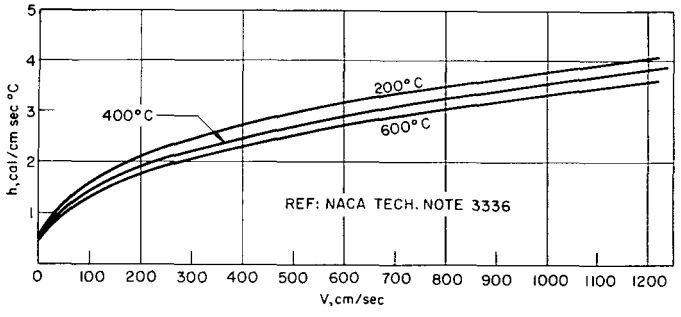

Fig. 5. Heat Transfer Coefficient for NaK 22 Wt % Na

The coefficient of heat transfer as a function of NaK velocity with NaK temperature as parameter is shown in Fig. 5.

(c) Elasticity

The radial spacers between the rods assure that the center lines of the rods remain essentially in the same relative positions and that the force of thermal expansion is expressed as strain energy in the metals of the core. As the temperature of the metals increases, there is a compression of the rods and spacers but a stretching of the structure containing them. Concurrently, the volume of the uranium increases, the volume of NaK decreases, the velocity of the NaK increases, the convection heat transfer rate increases, the microscopic cross sections of isotopes change, and there is a Doppler effect. All of these have an effect upon reactivity. The significant effects are due to variations in core volume and NaK density.

The effect of axial expansion is that of increasing the length of the rods and of the structure. The rods at the center of the core will try to expand more than the rods at the periphery. Any plane which was perpendicular to the center line of the core axis during the steady-state condition, except that plane through the peak of the neutron buckling along the axis, will appear as a surface of revolution during the change in power and possibly afterwards.

The actual expansion of any rod is dependent upon its thermal condition and upon the restraining effect occasioned by contact with adjacent rods or shell, as each rod attempts to move through the compacted bundle of rods.

The amount of restraint depends upon the interface contact pressure between adjacent longitudinal elements. This pressure is due to manual clamping and to restrained radial thermal expansion. Throughout

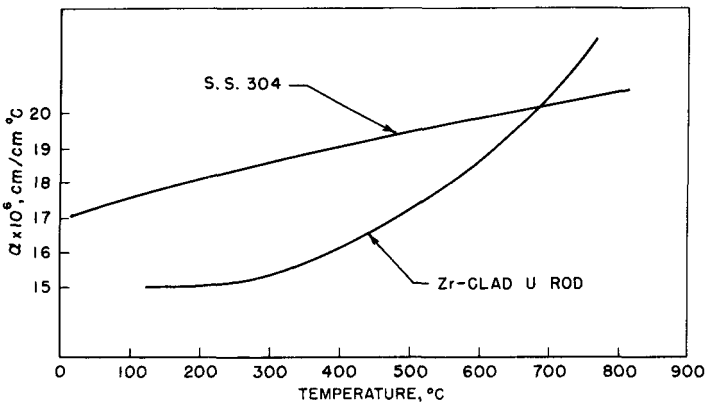

Fig. 6. Coefficients of Thermal Expansion

the range of temperature of materials, the coefficient of expansion of stainless steel is greater than the equivalent coefficient of expansion of the bimetallic rod (Fig. 6).

The coefficient of expansion of stainless steel is nearly constant over the range of temperatures to which it is subjected, but the coefficient of uranium varies widely over the range of temperatures. The coefficient of uranium was expressed as a function of temperature in the model.

The restraining effect of the cladding upon the radial and axial expansions was considered first and then the effect of the radial spacers.

The uranium rod is clad with a drawn-on zirconium tube. The absolute temperatures in the uranium are higher than those in the zirconium, and the coefficient of expansion of the uranium is approximately three times that of the zirconium ($\alpha_u \cong 3\alpha_z$). The uranium will be in compression and the zirconium in tension. Strain-energy methods were used to determine how much the uranium could expand against the restraining influence of the zirconium. Equilibrium exists when the strain energy of the uranium equals the strain energy of the zirconium, and the increases in length and diameter of the uranium and zirconium will be those concomitant with this condition.

The clad rod presents a three-dimensional problem in elasticity. However, in the interest of simplicity it was treated as a two-dimensional plane strain and an axial strain problem.

The expansion of the uranium in the bimetallic rod provides all of the driving force and part of the retarding force associated with the movement of the uranium.

The radial movement of the uranium, retarded only by the zirconium cladding, was determined from the condition that the increase in radius of the zirconium must equal the decrease in the outer radius of the uranium.

The difference in radius (δ) of the uranium and zirconium from that which it would have been if both rod and cylinder were permitted to expand fully was determined by equating the strain energy in each:

$$V_u = V_z \quad .$$

Now,

$$V = \frac{1}{2E} (\sigma_r^2 + \sigma_t^2) - \frac{\nu}{E} \sigma_r \sigma_t + \frac{1 + \nu}{E} \tau_{rt}^2 \quad . \tag{6}$$

The boundary conditions are that σ_r equal the pressure at the interface of the U rod and Zr cylinder and that the derivative of σ_r with respect to r is zero at the center of the U rod.

$$\Delta r/r = (\alpha T)_u - \delta \tag{7}$$

$$\Delta r/r = (\alpha T)_z + \delta \tag{8}$$

$\Delta r/r$ provides a clamping force in the core and blankets, which is a function of the thermal conditions in the reactor. The summation of $\Delta r/r$ is $\Delta R/R$.

The axial movement of the uranium retarded only by the zirconium cladding is determined in a similar manner.

The unit elongation of both uranium and zirconium must be the same.

$$x_f = \frac{\Delta \ell}{\ell} = \frac{(\alpha A E \Delta T)_u + (\alpha A E \Delta T)_z}{(A E)_u + (A E)_z} \tag{9}$$

The effect of the radial spacers is that of holding the relative spacing of the fuel rods nearly constant. As the rods tend to bend or buckle, they are restrained by these radial spacers. The structural system of the Mark-III core is statically indeterminate and the shape of the centerline of a rod is that concomitant with energy equilibrium. The contact pressure between a zirconium spacer and fuel rod causes a much greater relative decrease in diameter of the spacer and thus greater stress. The spacers would be the first to be compressed beyond the elastic limit as the temperature gradient increased. As long as the temperature gradient is such that the spacers are not compressed beyond the yield point, the bundle of cylinders will return to its original position with point contact between parallel cylinders. If the rod is restrained, reactive couples along the length of the rod try to reduce the curvature due to nonuniform heating (Fig. 7).

The strain energy in a spacer rod is the sum of that due to the bending moment and that due to the radial pressure. If two elastic objects with convex surfaces are pressed against each other in the direction of their common normal, their respective surfaces become flattened and high local

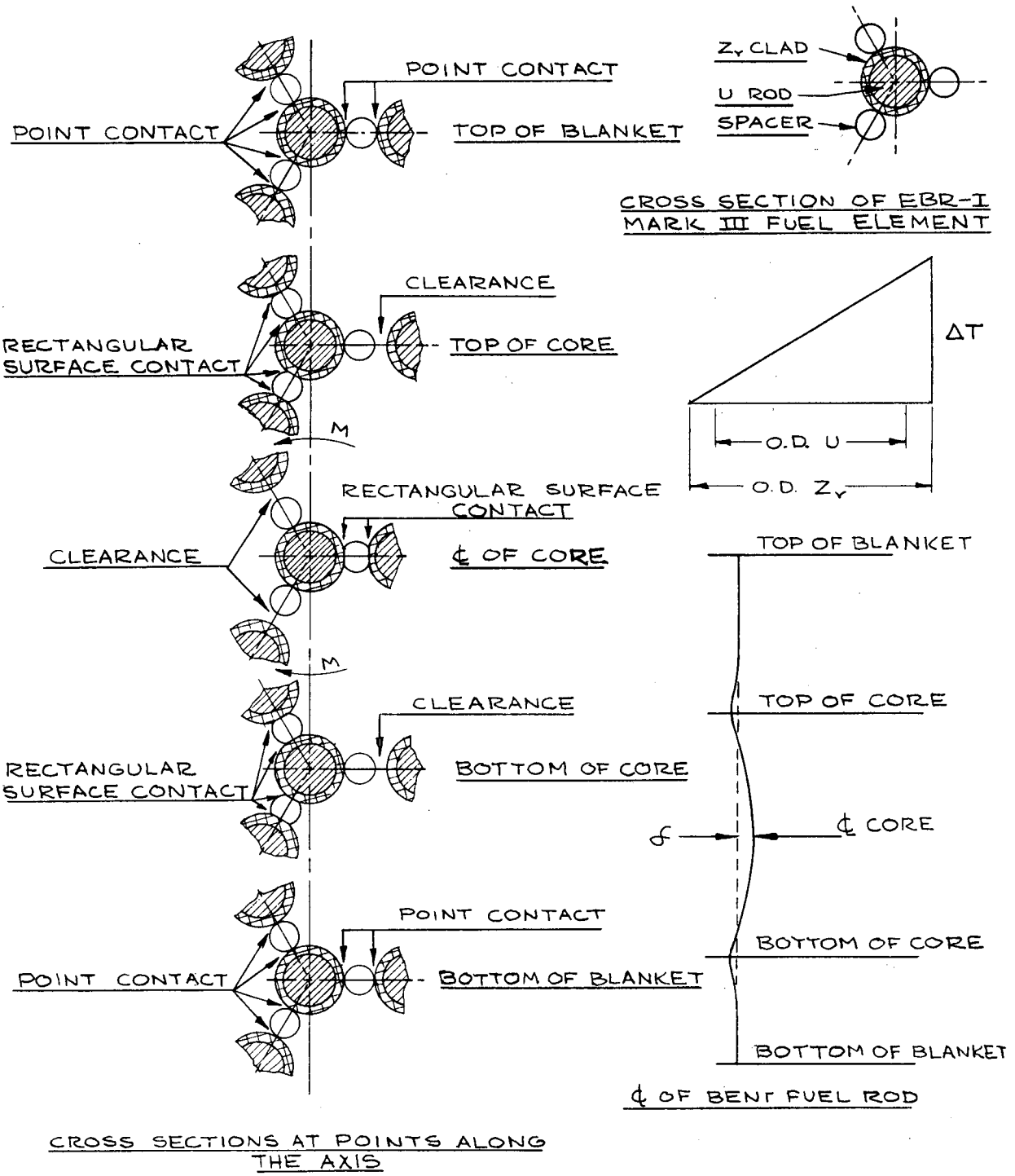

Fig. 7 Effect on Zr Spacers of Bending Moments due to Diametrical Temperature Gradients

stress is present. In the case of the rod and spacer the contact surfaces are narrow rectangles of a width (2a) which is a function of strain energy in the rods:*

$$a = 1.522 \sqrt{\frac{P r_1 r_2}{E(r_1 - r_2)}} \qquad (10)$$

where r_1 is the radius of rods and r_2 is the radius of spacers. This rectangle of width 2a is the contact surface with adjacent rods and structure. The pressure, P, is determined from a synthesis of test results. It was a question of determining how tight was tight.

(d) Nonlinear Mechanics

If the heterogeneous assembly of materials comprising the core and blankets and contained in the stainless steel shell expanded freely, the axial movement of a rod would be $X_f = \Delta\ell$; but there is mechanical restraint, so the movement is some other value, X, which is X_f retarded in time and modified in magnitude.

An oscillation of the forcing functions causes this assembly of materials to expand and contract alternately. The mechanical restraints in the form of friction phenomena constitute the damping in the forced oscillation of a redundant elastic structure.

Since bowing and elastic buckling are obviously of little consequence in this particular reactor, the nonlinear effects must be due to mechanical restraints and friction phenomena. The mechanical restraints are due to friction between rods moving relative to each other and to their containing structure. The normal force in the friction phenomena is due partially to initial manual clamping, a relatively small effect, and to radial thermal expansion.

When the bundle of rods becomes hot, there is random thermal distortion and contact between adjacent rods and between rods and structure. Since the bundle of rods is clamped circumferentially, an increase in $\Delta r/r$ of each rod further increases the normal forces at the surfaces of contact and thus increases the resistance to relative movement of rods and structure. Thus the free response to thermal forcing functions is modified.

It would be impractical to try to take into account the exact movement of every unit volume of the core. Therefore, a dynamically equivalent model of core and blanket must be used. It was considered that the dynamic characteristics of the variations in core and blanket dimension can be simulated by analogy to single rods in a tightly bound bundle of rods. While this is not a refined analogy physically, it is good dynamically, and the constants associated with the equivalent friction phenomena are physically plausible.

*Nadai, Theory of Plasticity, McGraw-Hill, New York, N.Y.

It is apparently a correct analogy as the reactor and model are dynamically similar for all operating conditions, as evidenced by the spread and configuration of the curves in Figs. 10-13, the correspondence of reactor and model responses to a rod drop at power, Figs. 25a, b, c, d, the agreement in magnitude of hysteresis in the reactivity vs power curve, Fig. 14, and the correspondence between sinusoidal responses, Figs. 26a-i.

A rod is represented by a series of segments of mass m separated by springs which represent the modulus of elasticity of the rod (Fig. 8). The force of thermal expansion is manifest as a change in the equilibrium length of the springs. The movement of each mass is retarded by the friction force dragging on its surface. The equation of motion of a mass m is considered to be that of a simple harmonic oscillator with static and sliding coulomb friction forces added.

$$m\ddot{X} = \frac{gEA}{\ell} (X_f - X) - c\dot{X} - F - F_r \qquad (11)$$

For $0 < \dot{X} < \epsilon$: $F_r = \mu_0 N$; $F = 0$,
For $\dot{X} > \epsilon$: $F_r = 0$; $F = \mu N$

The velocity $\dot{X}$ is very fast compared to the velocity $\dot{X}_f$, so that essentially $\dot{X}_f$ is zero compared to $\dot{X}$. When the mass m breaks loose, it jumps and it may or may not overshoot, depending on the relative magnitudes of the frictional forces.

A mass m will not move until the force resulting from thermal expansion is equal in magnitude and in opposition to the static coulomb friction, F_r. The mass then breaks loose and moves rapidly against a combination of sliding coulomb and viscous friction until the combined force of these brings the mass to rest. At this condition, F_r is again greater and the mass sticks. The cycle is repeated until X_f changes sign and the cycle of friction phenomena reverses.

The power response of the model to a given signal is shown for a number of operating conditions (Fig. 9a, b). It is obvious that the nonlinear effects are present. The equivalent rod is stuck at point "A" (Fig. 9b) and does not build up enough expansive force to move until the power level has risen to point "B." At point "B" the rod breaks loose and moves forward at high velocity, so the power drops to that indicated by point "C," due to the introduction of negative reactivity. At "C" the sticking force is greater than the expansive force and the mass is stuck again. This cycle repeats and reverses at point "G."

If the friction forces are zero, there is no mechanical interference and $(X_f - X)$ is zero.

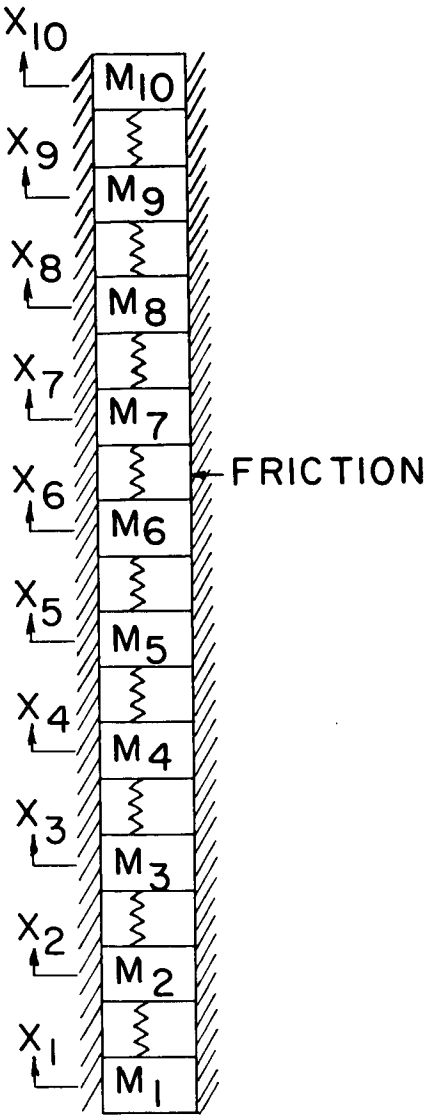

$$m\ddot{x} = \frac{gEA}{\ell}\,(X_f - X) - c\dot{X} - F - F_r$$

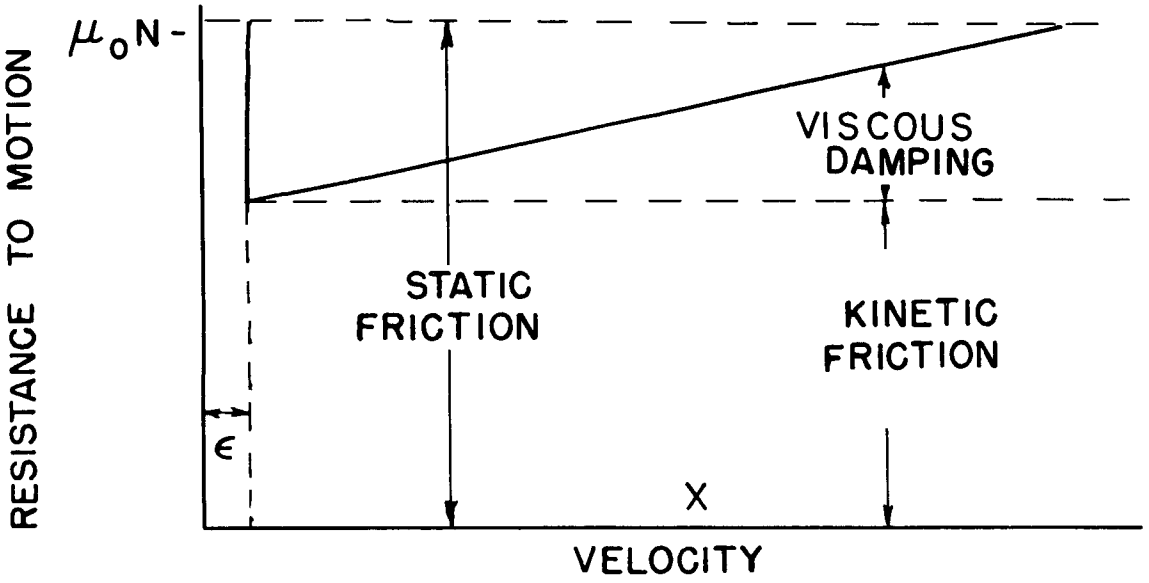

Fig. 8. Equation of Motion of a Rod

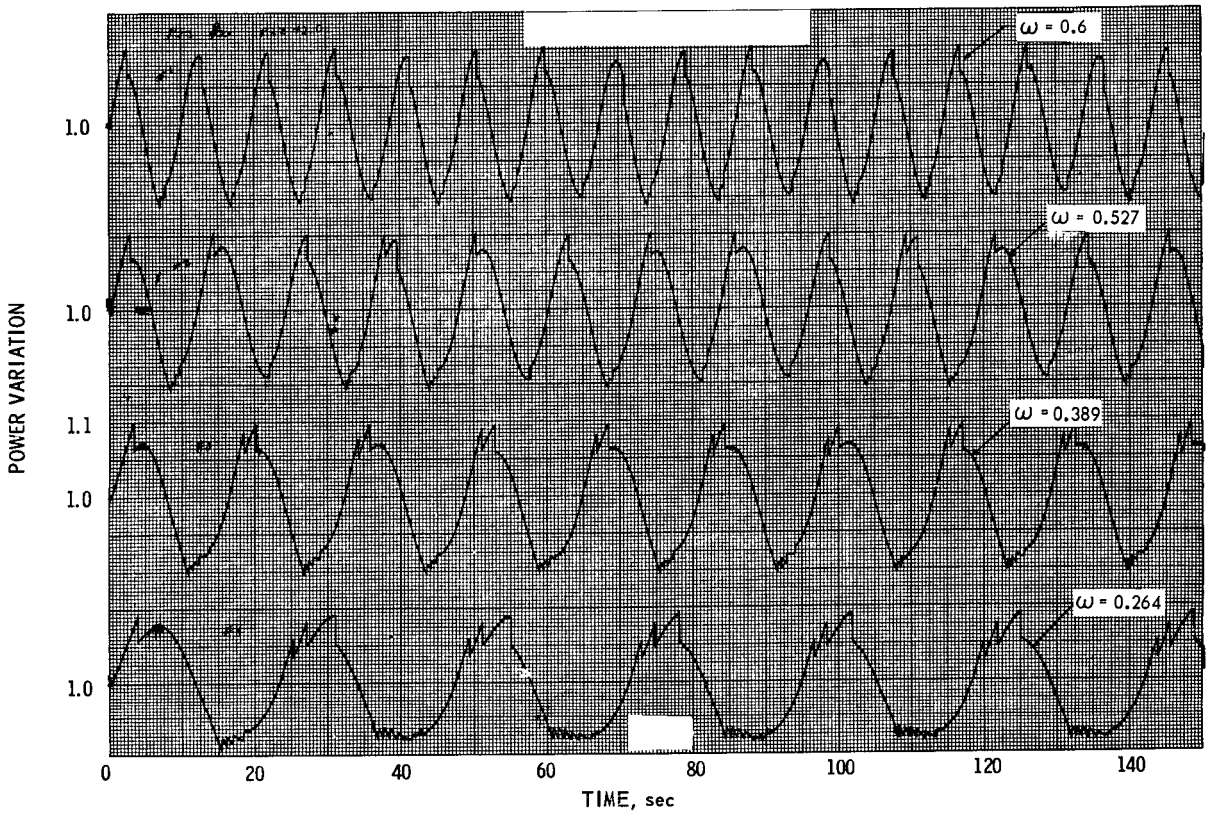

Fig. 9a. Total Response to Sinusoidal Signals

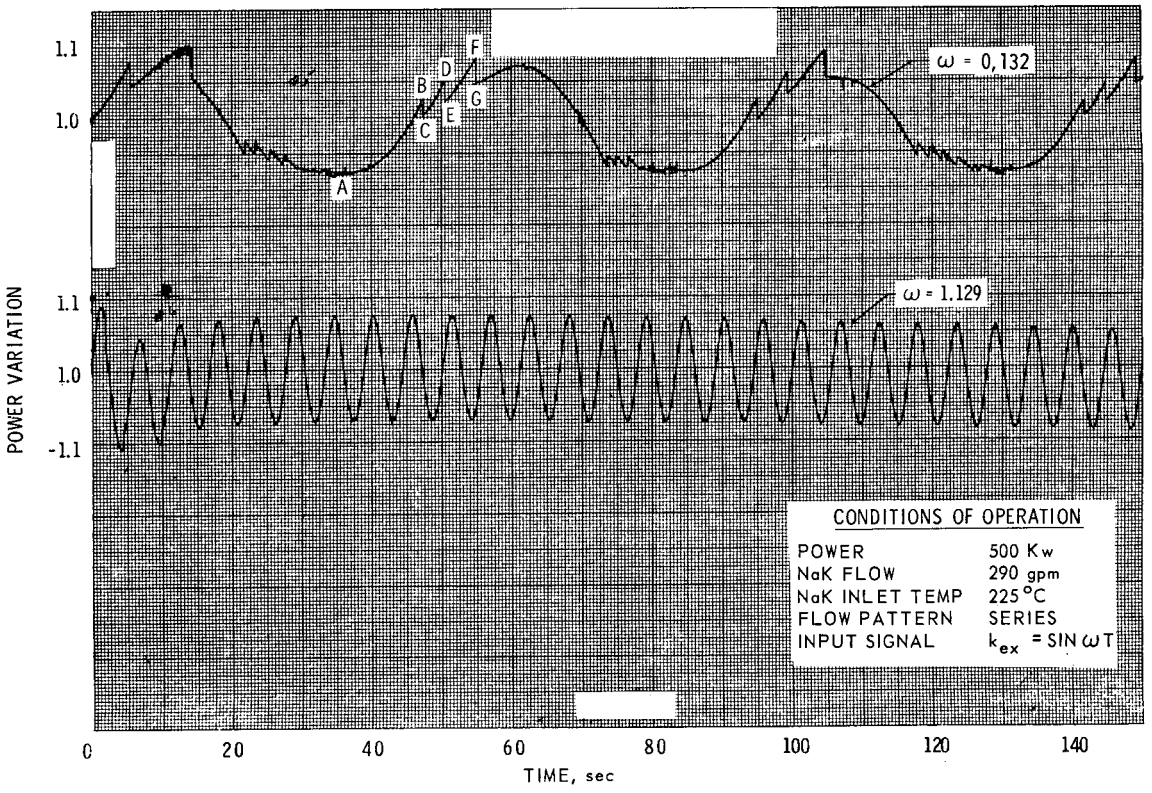

Fig. 9b. Total Response to Sinusoidal Signals

The quantity X_f is a function only of temperature in the rod and its zirconium cladding. It is independent of the position of the mass m. The frictional force exerted by the surfaces in contact is assumed to be directly proportional to the total normal force acting on the surface of contact. The interface pressure is a very complicated function of rod temperature. It has been reduced to an equivalent simple expression for $\Delta r/r$. The total frictional force is assumed to vary with mass velocity, $\dot{X}$, as shown in Fig. 8.

The total normal force N on the surface of a rod is expressed as

$$N = F_c + C_f (\Delta r/r) \quad , \tag{12}$$

in which F_c is a constant normal force (due to the original manual clamping of the rods), and C_f a constant of proportionality relating a radial thermal expansion of the mass m to the resulting change in total normal forces. Thus

$$F = \mu N = \mu [F_c + C_f (\Delta r/r)] \tag{13}$$

Dividing equation (11) by ℓ to facilitate use in the analog circuitry,

$$m\ddot{x} = \frac{gEA}{\ell} (x_f - x) - c\dot{x} - \frac{F}{\ell} - \frac{F_r}{\ell} \quad . \tag{14}$$

For qualitative understanding of the equation of motion, consider x_f as a constant. Motion will start when the expansive force equals the static friction force ($F_r = \mu_0 N$). From the well-known motion of the linear simple harmonic oscillator, it can be seen that after motion starts the magnitude of the expansive force will always be less than its initial value ($\mu_0 N$) regardless of the values of the coefficients. The mass m will then stick at the instant that $\dot{x}$ passes through zero for the first time after starting. Under these conditions, the motion of m is a series of jumps or steps beginning whenever the expansive force, $(gEA/\ell)(x_f - x)$, equals $\mu_0 N$.* Again drawing upon familiarity with the simple harmonic oscillator equation, it can be seen that motions corresponding to all possible values of the system coefficients must fall into two categories: either the jump undershoots the equilibrium point, $x_f - x = 0$, or overshoots by an amount not greater than the initial offset, Δx_0. As mentioned before, the movement x will be a series of jumps or steps. The steps will have a rise time determined by ω_0, the undamped natural frequency assumed for the equivalent mass-spring system. This is taken as the frequency of the fundamental mode of longitudinal vibration of the uranium rods,** which is

*Hass, V. B., Jr., Coulomb Friction in Feedback Control Systems, Trans. AIEE, Vol. 72, Part II (1953)

**Timoshenko, Vibration Problems in Engineering, McGraw-Hill, New York, New York (1937), second edition.

approximately 4,000 cps. The analog circuit for the system makes use of the fact that the response of any system to a step is independent of the rise time of the step so long as it is short compared to any of the significant time constants of the system. In the analog circuit for the equivalent mass-spring system, the time scale was slowed by a factor of 800, so that the value of ω_0 used in the analog was 5 cps, making the rise time of the steps just short enough to satisfy the above requirement.

At the instant of slipping, the expansive force equals the static coulomb friction:

$$(gEA/\ell)\,(X_f - X) = F_r = \mu_0 N \qquad (15)$$

The unit strain $(X_f - X)/\ell$ at the instant of slip is defined as Δx_0, the slip level. Then

$$(gEA/\ell)\;\ell\Delta x_0 = \mu_0 N$$

or

$$\Delta x_0 = \mu_0 N/gEA \qquad (16)$$

The motion after slipping is considered to be the same as that of a linear second-order system responding to an initial unit strain $\Delta x_0'$ which is less than Δx_0 by an amount equivalent to the kinetic coulomb friction force, F:

$$\Delta x_0' = \Delta x_0 - (F/gEA) \qquad (17)$$

The motion of the non-linear system responding to an initial offset Δx_0 is then identical to the motion of the system, with F = 0, responding to an initial offset $\Delta x_0'$. This condition is true until $\dot{x}$ returns to zero (that is, $<\epsilon$) for the first time after slipping occurs.

The movement x of the system for F and F_r equal to 0 is given by the solution of the eq. (14) for a unit step input, which is

$$x = 1 - e^{-at}\left\{\frac{a}{b}\sin bt + \cos bt\right\} \qquad (18)$$

in which

$$a = c/2m; \qquad b = \sqrt{\frac{k}{m} - \left(\frac{c}{2m}\right)^2}; \qquad k = gEA/\ell;$$

$$\dot{x} = \frac{k/m}{b}\, e^{-at} \sin bt. \qquad (19)$$

The first zero of eq. (19) occurs at the time

$$t = \pi/b \quad .$$

Inserting the value of t in equations for x,

$$x_{(\dot{x}=0)} = 1 + e^{-a\pi/b} \quad . \tag{20}$$

This is the position at the instant that mass m comes to rest for the first time and is the position at which it sticks in the nonlinear case.

The magnitude of an individual jump Δx is:

$$\Delta x = (\Delta x_0') \, x_{(\dot{x}=0)}$$

$$= \left(\Delta x_0 - \frac{F}{gEA}\right) x_{(\dot{x}=0)}$$

$$= \frac{\mu_0 N}{gEA}\left(1 - \frac{1}{\alpha}\right)\left(1 + e^{-a\pi/b}\right) \quad . \tag{21}$$

The amount of movement in terms of the relative jump, δ, is:

$$\delta = \frac{\Delta x}{\Delta x_0} = \left(1 - \frac{1}{\alpha}\right)\left(1 + e^{-a\pi/b}\right) \quad . \tag{22}$$

There is no apparent way of estimating the actual value of c. The value for critical damping was used:

$$c_c = 2\sqrt{km} \quad .$$

In this case δ is a function only of the ratio of static to kinetic coulomb friction:

$$\delta = 1 - \frac{1}{\alpha} \quad .$$

The value of δ which fits the actual reactor responses corresponds to $\alpha = F_r/F = 3.3$.

The character of the response of a system of this type is best presented in terms of the damping ratio, ζ

$$\zeta = \frac{c}{c_c} = \frac{c}{2\sqrt{km}} \quad .$$

Thus

$$c = 2\sqrt{k\,m}\;\zeta$$

$$a = \sqrt{k/m}\;\;\zeta$$

$$b = \sqrt{k/m}\;\;\sqrt{1 - \zeta^2}$$

$$a/b = \zeta / \sqrt{1 - \zeta^2} = \lambda \quad .$$

Equation (20) then becomes

$$x_{(\dot{x} = 0)} = 1 + e^{-\lambda\pi} = f(\zeta) \quad .$$

Since α in the real system may vary from 0 to $+\infty$, and $f(\zeta)$ from +1.0 to +2.0, the relative jump, δ, can vary from 0 to 2.0. The values of α and ζ affect only the rise time of the jump, which, as stated earlier, is of little consequence, since it is always extremely fast compared to the reactor responses.* Hence, the reactor would be insensitive to different values of α and ζ for the same relative jump.

In the analog circuitry for solving the equation of motion (14), it was found convenient to set ζ constant at 1.0 and to vary the relative jump in the range 0 to 2.0 by means of a coulomb friction force term in which the polarity was reversed to produce overshoot or relative jump in the range between 1.0 and 2.0.

The assumption was made that α and ζ do not vary with radial pressure or temperature; hence, the relative jump is a constant to be determined by analog experimentation to fit the actual reactor responses. The unit expansive strain at which slip occurs is a function of rod temperature, in virtue of the dependence of N on radial thermal expansion. Thus, the constants F_c and C_f and the relative jump δ represent three degrees of freedom by which it is possible to match the responses of the model to those of the actual reactor. Once these constants in the nonlinear equations were established, they remained fixed from then on. Only the operating conditions were varied to correspond with those of the reactor. The constants so determined were reasonable for friction phenomena (Appendix B). The constants listed in Appendix B were determined by analog experimentation to fit Mark-III data at a coolant inlet temperature of 225°C. It is considered impossible at this time to evaluate friction phenomena in such a complex system in any other way.

---

*Qualification of this statement is in order since the prompt neutron response probably does follow such rapid steps in δk. The prompt response is so fast compared to the delay group time constants and thermal time constants that it may be considered to scale factor which converts the step in δk to an equivalent step in neutron density which is applied to the delay group equations and thermal equations.

The earlier statement that rise time of the jumps is very fast compared to reactor responses also leads to the fact that responses due to friction mechanisms are completely independent of the frequency of reactor oscillations, being dependent only on the amplitude of x_f. Hence, any frequency dependence (either in phase or amplitude) required of the unknown mechanism relating Δk to x_f must come about by virtue of the frequency dependence of the x_f amplitude. This emphasizes the fact that the frequency response or describing function of the feedback mechanism will be dependent on power level and amplitude of k_{ex} input. Hence, closed-loop frequency responses measured at different power levels and/or input amplitudes will dictate different transfer functions for $\Delta k/x_f$.

The analog circuitry included a term to take into account that fraction of $\Delta\ell/\ell$ which would appear with no time delay, which is due to elastic deformation of the core before actual slippage occurs between rods. The hot center core rods will expand, stretching the cooler blanket rods. The amount of deformation is that concomitant with elastic equilibrium. This provides a negative prompt $-\Delta k$ feedback term which would merely subtract from any prompt positive term if one were present.

The model is based on an equivalent rod model of the core. Actually, the core consists of many rods. The slip levels for each are likely to deviate slightly about some mean value. Because of this, the exact instant at which the various rods slip will be random; hence, the feedback will appear in very small discrete jumps as each rod moves. The time of slipping would be sufficiently random that the total feedback would appear almost as a smooth continuous function. While the exact time of slip varies for each rod, the individual effective phase lag and amplitude of response to a sinusoidal driving signal would be the same for all rods and hence the phase and amplitude of the equivalent rod model used in the analog is equivalent to the composite effect of all rods. The feedback from the equivalent rod appears in large jumps which show up in the closed loop response due to the prompt neutron response. (Figs 9a and 9b).

NONLINEAR CHARACTERISTICS OF THE REACTOR

Evidence of nonlinearity is shown in Figs. 10-13, where the amplitude of H was power normalized to the highest power. The spread in the family of curves of phase angles and power-normalized amplitudes indicates that H involves a nonlinear mechanism; otherwise power normalizing would make the amplitude curves coincident, and the phase would be independent of power.

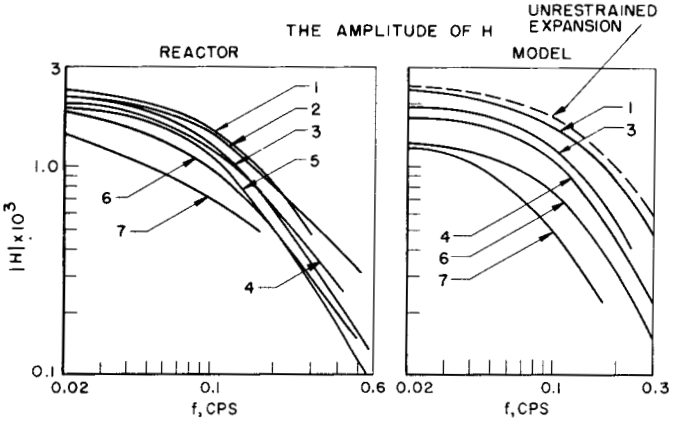

Fig. 10
Response to Sinusoidal Signals

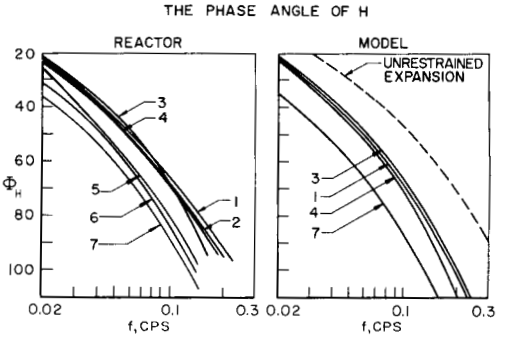

Fig. 11
Response to Sinusoidal Signals

NOTES
1- H NORMALIZED TO H AT 1150 kw
2- NaK FLOW=300 gpm (SERIES)

CURVE NO.	POWER, kw	OSCILLATOR ROD
1	1150	NEW
2	952	NEW
3	877	OLD
4	877	NEW
5	655	OLD
6	489	OLD
7	370	OLD

Additional evidence of nonlinearity is shown in curves 3 and 4 of Figs. 10 and 11, which are not coincident although they represent H for exactly the same conditions of reactor operation. The only difference is in the reactivity worth (inhours) of the rods (old = 9.8 sin ωt; new = 6.6 sin ωt).

It is to be noted that the corresponding model response curves spread in the same direction and by approximately the same amounts. The amount and direction of spread will not necessarily be correct simply because the model is nonlinear, and such was the situation in this analysis.

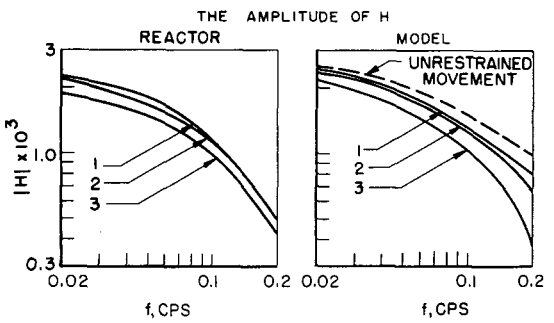

Fig. 12

Response to Sinusoidal Signals

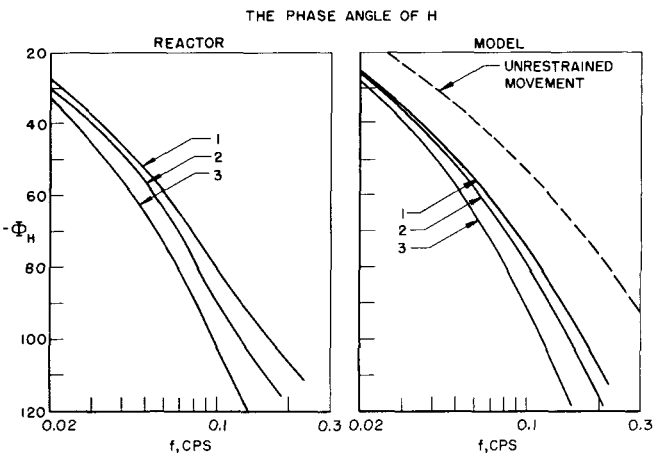

Fig. 13

Response to Sinusoidal Signals

NOTES
1 – H NORMALIZED TO 900 kw
2 – NaK FLOW, 180 gpm (PARALLEL)

CURVES	POWER, kw	OSCILLATOR ROD
1	900	NEW
2	738	NEW
3	500	OLD

Before the tests, the model was giving a nonlinear response, but about all that can be said for it was that it decreased the amplitude of the feedback and increased the lag angle. This was only a qualitative answer, but a step nearer to accounting for the actual response that linear analysis can give.

Upon receipt of the low-power test data, the constants in the mechanical motion equations were re-evaluated and throughout all further model operation they remained constant. The constants were not changed once they were determined.

The dashed lines on the amplitude and phase angle curves are the values for an H' corresponding to the completely free expansion of the core. Since the NaK transport velocity is constant, the thermal phenomena are approximately linear over the small temperature range involved in these experiments, and all power-normalized values of H' will be coincident with the dashed line.

Linear analysis of this reactor at these velocities of 300 gpm and 180 gpm may give an H' which matches one of the values of H (Figs. 10-13), but H' can match only one.

A further property of the nonlinear feedback is that the reactivity vs power curve shows a hysteresis effect.* The reactor follows one curve of steady-state feedback of reactivity vs power when going up in power and follows another curve parallel to, but above, the first curve when coming down in power.

The movement of a mass (Fig. 8) lags the driving force by the amount of time required for the driving force to equal the Stiction force. In one case the mass is moving from a low-temperature base and in the other case the mass is moving from a high-temperature base. The rod tends to remain at a length concomitant with the temperature base. Figure 14a shows the actual variation of reactivity with power in the model and in the reactor for a monotone increase of power from zero to maximum power, then a monotone decrease in power to zero. Figure 14b is a magnification of this to illustrate the effect of slip level and relative jump. The center line in Fig. 14b is the reactivity due to unrestrained expansion. The dashed lines above and below this are displaced vertically from it by an amount "A" times Δx_0, the slip level for the equivalent rod; "A" is a constant relating motion to reactivity. The reactivity at a given power will always be between the slip level line and a line displaced from the latter by the amount of the jump, $A\ \Delta x_0 \delta$. Points corresponding to randomly chosen powers will fall anywhere in the stick-jump cycle between these extremes with equal probability. The average location in the cycle will then be midway between the extremes. If there is sufficient randomness in the slip levels of the individual rods, the locations of each of the rods in their individual cycle at a given power will be random. Further, assuming applicability of the Central Limit theorem, which states that the ensemble average at one power equals the individual rod average cycle location over all powers, it follows that the total Δk from all rods would follow a smooth curve midway between the average slip level and the line displaced from it by the average jump.

*This is evident in the data of Progress Report #2 on EBR-I, Mark III. In all subsequent data the hysteresis effect was lost by shutting the reactor down between increasing power and decreasing power experiments, except for a single point shown in Fig. 14e.

Thus, the actual reactor shows a curve of reactivity vs. power in the form of a hysteresis loop in which the vertical displacement between the ascending and descending power branches is given by

$$D_h = 2A\,\Delta x_0\,(1 - \tfrac{1}{2}\,\delta) \quad .$$

Using values of δ and Δx_0 for coolant inlet temperatures 225°C, there results

$$D_h = \frac{2(1.82)\,(0.12 \times 10^{-4})\,(1 - 0.70/2)}{0.226 \times 10^{-4}} = 1.3 \text{ inhours.}$$

The power-reactivity curves show two other unexpected features. Typical examples are shown in Figs. 14c, d, e.* One of these features is the nearly zero slope below about 100 kw. This is apparent only in Fig. 14c, since normalization removed the effect from other data. The second is a small decrease in slope occurring at about 500 kw at low NaK inlet temperature, say 70°C, and around 800 kw at 240°C. This is evident in Figs. 14d and e.

It is believed that these two effects may have resulted from small residual clearances existing between rods and spacers at random points along the rods throughout the core. Due to random warping of the rods, such clearances could exist at some points while other points are tight. As power is increased from zero, the rods would first bow inward due to radial temperature gradient and axial compression until these clearances are taken up. The resulting positive term would reduce the net negative feedback in the region from 0 to 100 kw. At 100 kw all rods have moved inward as far as the residual clearances will allow, and thus the positive term is limited at this point. Above 100 kw the positive feedback vanishes.

At about 500 to 800 kw, depending on coolant inlet temperature, radial expansion has completely taken up all residual clearances. Radial motion of the fuel rod centerlines ceases, and only the diameter increases, thereby flattening the spacer wires. This limits the negative feedback term due to radial expansion, producing the reduced slope of the curve at high power.

This mechanism for explaining the changes in slopes of the reactivity curves is at present not included in the model, as it would have little effect other than to change the total feedback gain proportionately. The exact value of the latter is at the moment somewhat in question due to uncertainty in the flow partition between blanket, core, and bypass leakage. It is, of course, necessary to know the exact flow distribution in order to predict reactor responses accurately. Furthermore, this mechanism of residual clearance causing slope changes is still in the form of conjecture, having not yet been subjected to any quantitative test.

*Progress Report #2, Fig. 11. Results of Parallel Flow Studies, Smith, Boland and Thalgott (April 17, 1958). Progress Report #7, Tables X and XI, Results of Oscillator Studies EBR-I Mark-III, Smith, Boland, and Thalgott (December 22, 1958).

The hysteresis effect caused by restraint of expansion, however, is in surprisingly good agreement with the measured data as shown in Fig. 14a. The constants of the damping mechanism were not changed from the values used in the sinusoidal experiments described previously.

The Mark-III data shown in Fig. 14a have been increased by 10 inhours, the amount of the apparent limited positive feedback term, so that they fall along the model curve which does not include this term. This was done to demonstrate the agreement both in slope and hysteresis.

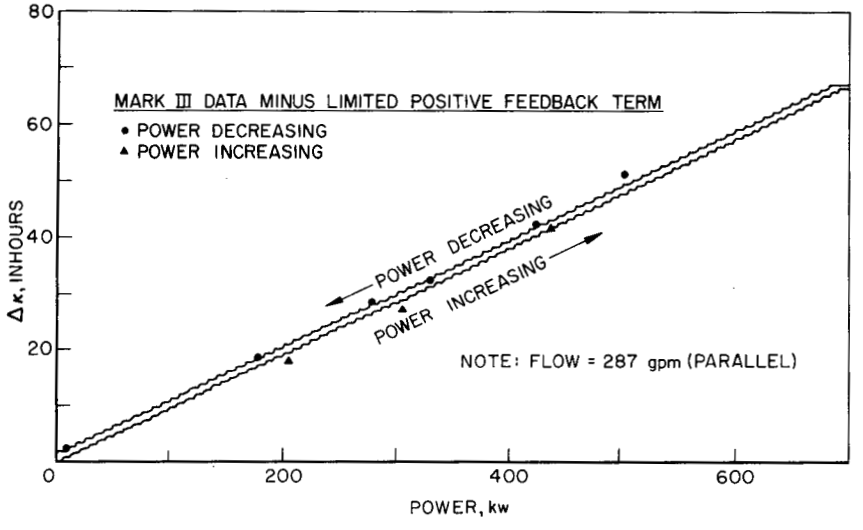

Fig. 14a

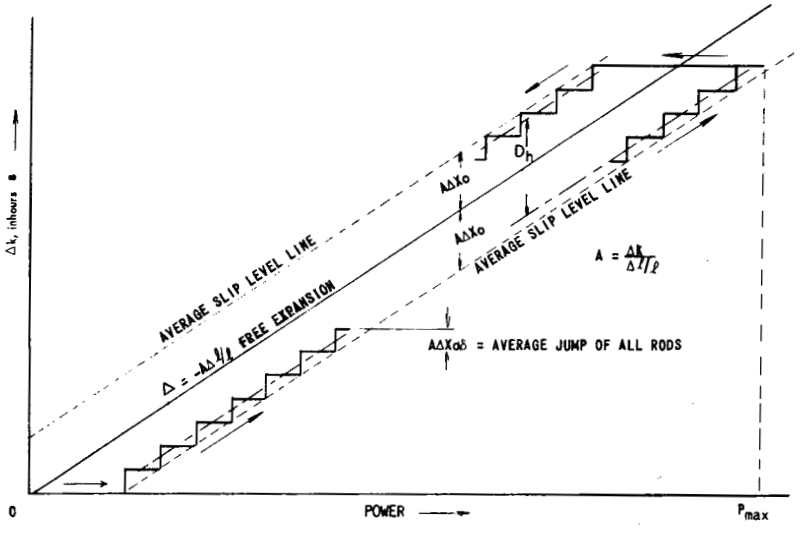

Fig. 14b

Fig. 14 Open Loop Δk vs Power

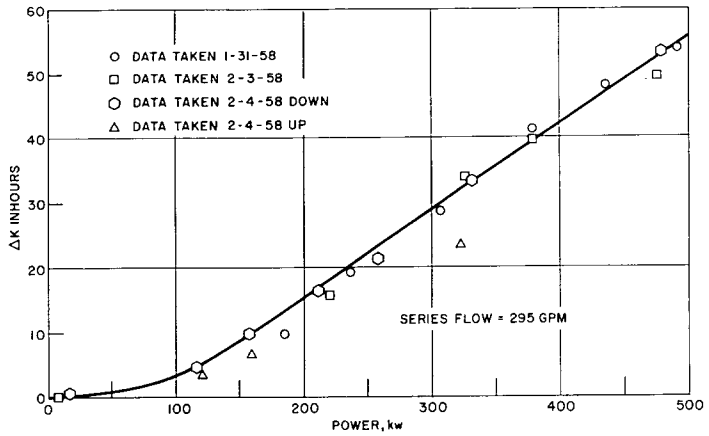

Fig. 14c

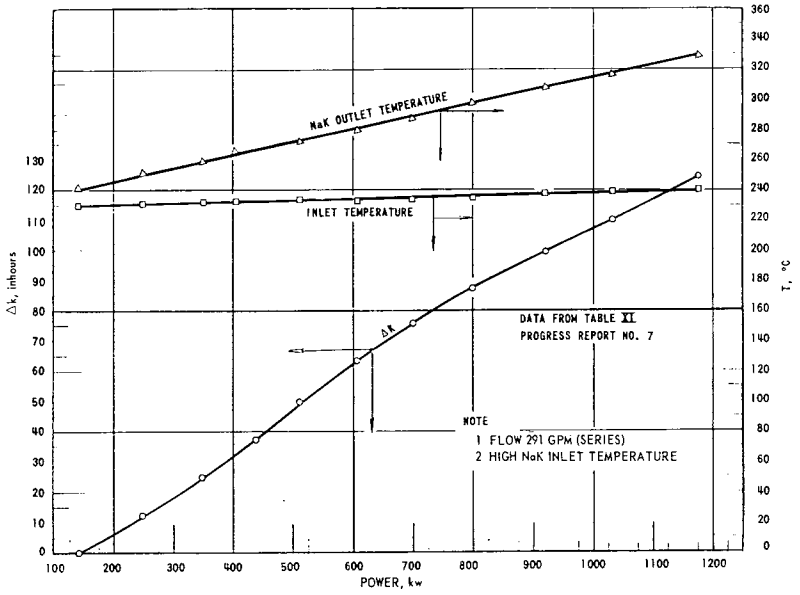

Fig. 14d

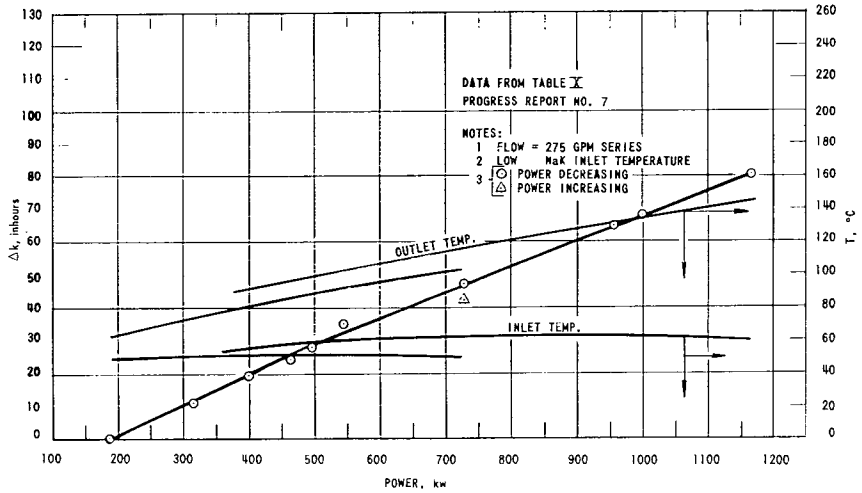

Fig. 14e

Fig. 14 Open Loop Δk vs Power (Cont'd.)

Variation of Feedback Gain with Coolant Inlet Temperature

While it has not been done yet, it appears likely that a physically plausible variation in tightness with temperature can be found to produce the observed variation of feedback gain with inlet temperature without changing the present constants in the equation of motion, at 225°C inlet temperature.

Figure 6 indicates that, due to greater expansion of the stainless steel shell below about 700°C, the tightness or slip level, Δx_0, would decrease as inlet temperature rises. It can be shown by Fig. 23 that, with decreasing slip level, the sinusoidal gain of the restraint mechanism increases. The curve for x/x_f vs. x_f given is valid for the slip level and relative jump of the model. If the abscissa was instead $x_f/\Delta x_0$, the curve would be valid for any other model having the same relative jump but any Δx_0. Hence by decreasing slip level, $x_f/\Delta x_0$ is increased, with corresponding increase of gain and decrease of phase lag as indicated by Fig. 23. Thus the restraint mechanism would cause feedback gain to increase with increasing inlet temperature. This is actually observed in Mark III.

The constants of eq. (11) used for the computer runs shown previously assumed that the tightness or Δx_0 was independent of power level. It can be shown that for the variation of fuel rod temperature encountered in the experiments described before at 225°C inlet temperature, the expected change in tightness is considerably less than would result from the large changes in inlet temperature used in the later experiments on effects of inlet temperature. This is because only a small fraction of the U in the reactor (the enriched part) changes volume appreciably on a change of power or flow. On changing coolant inlet temperature, every part of each rod in the reactor expands equally, giving a larger differential change of volume between the reactor tank and its contents.

It is apparent from the many simplifying assumptions which have been made in the foregoing analysis of this hypothesized restraint mechanism that the results can be regarded only as semi-quantitative. This mechanism is presumed to be the source of the unknown feedback delay observed in EBR-I. It is also believed possible by this mechanism to account for the observed nonlinearities in the reactivity vs. power curves, and for the variation in feedback gain with coolant inlet temperature.

EXPLORATION WORK WITH MODEL

In addition to operating the model at conditions simulating those at which the reactor was operated, the effect of the following was observed on the model.

1 - The Effect of Increasing the Magnitude of k_{ex}

For a sinusoidal input this was shown on Figs. 10-13 (curves 3 and 4). The effect of step inputs of reactivity from k_{ex} = 0.001 to 0.007 are shown in Fig. 15.

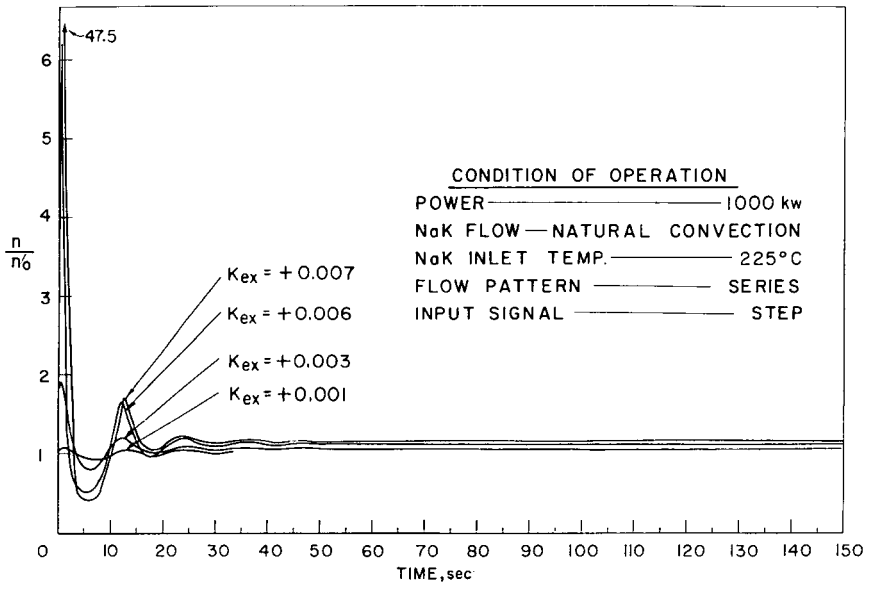

Fig. 15. The Effect of Increasing the Magnitude of the Steps in Reactivity

2 - Prompt Positive Feedback

It has been postulated that a small positive prompt feedback may be responsible for anomalies in the power reactivity curves (Figs. 14a, b, c, d). There is good evidence, judging by the shape of the power reactivity curve, that one does exist, but there is no reason to believe from an analysis of the physical features of Mark III and the test data that it can have any significant effect on the stability of the reactor.

If a significant positive feedback exists in a reactor, it should be obvious during a transient or excursion at high power and low coolant flow.

It is of interest to see if a prompt positive feedback capable of producing instability at high power and low flow can exist and not be detected in the response to oscillatory and step signals at normal conditions of operation. Therefore an arbitrary prompt positive feedback "A" was added to the feedback of the model. The results are shown on Fig. 16a, b.

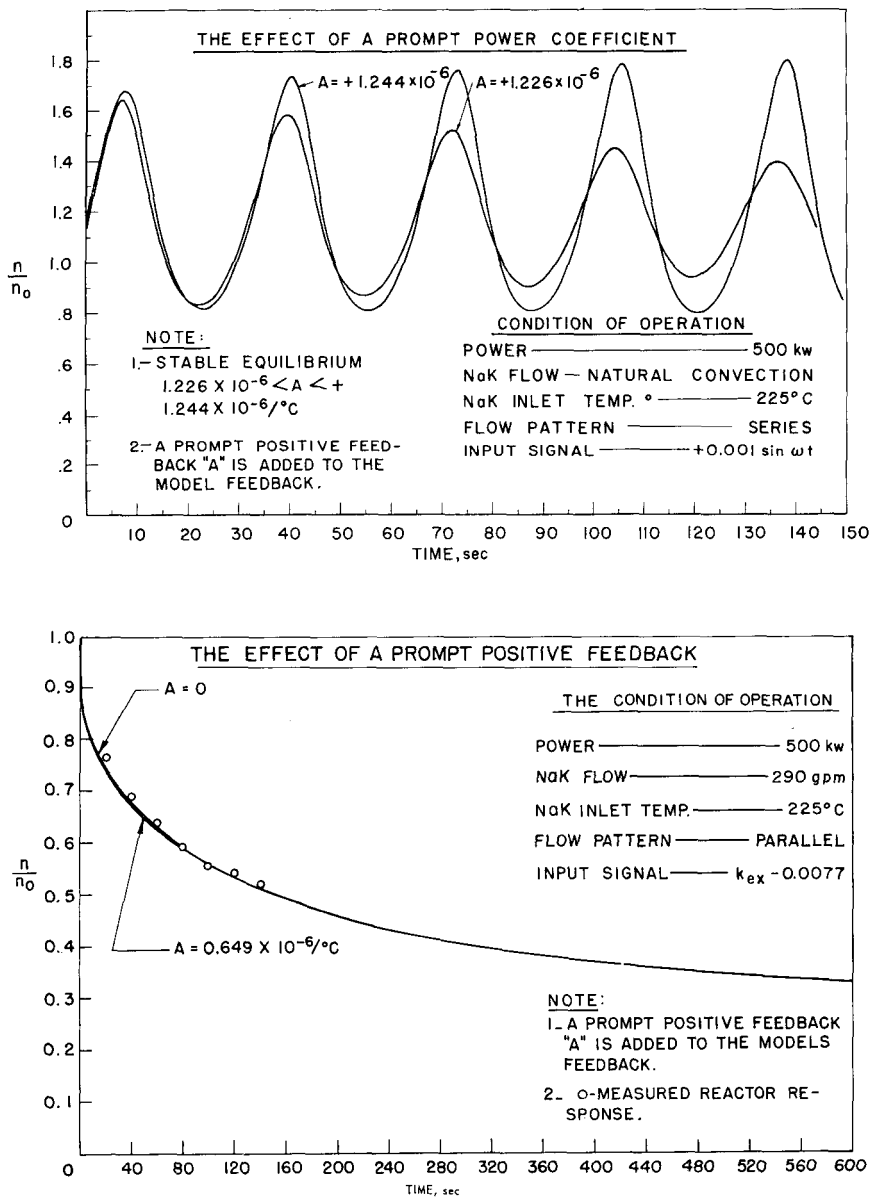

Fig. 16a,b. The Effect of a Prompt Positive Feedback

The quantity "A" can exist, not be obvious, and yet cause instability at operating conditions not impossible to reach during the course of normal operations. The value of "A" was increased until evidence of instability

appeared ($+1.226 \times 10^{-6}/°C$ < "A" < $+1.244 \times 10^{-6}/°C$). There does not appear to be any physical mechanisms in Mark III for attaining a significant positive feedback.

When ("A" $\leq +0.649 \times 10^{-6}/°C$) is added to the model's feedback for a rod drop insertion of $-k_{ex}$, there is little observable effect on the response, as shown in (Fig. 16b). The effect of the prompt feedback would only be evident early in the response to a rod drop insertion because the quantity s in the Laplace transform approaches zero rapidly.

Radial movement of uranium toward the center line of the core is considered to be the mechanism by which positive reactivity could be produced in the core;therefore in this reactor any positive reactivity feedback is very small compared to the negative feedback. If the radial spacers are removed from the core section in future experiments, the inward radial movement may be sufficient to cause significant positive feedback.

3 - High Gain

A high gain in a dynamic system is a cause of instability; therefore, increasing the feedback of negative k_{ex} will eventually produce instability in EBR I, Mark III. A step input of reactivity was used since it is the type of input most likely to initiate instability. The only way to attain a high gain is to increase the uranium temperature. An increase in temperature can be attained by increasing power and decreasing coolant velocity. The forced flow of coolant through the model is stopped; therefore, cooling is by natural convection, conduction and radiation only. Power is then increased until instability occurs. Instability of the model occurs at 32 times full power. The results are shown in Fig. 17.

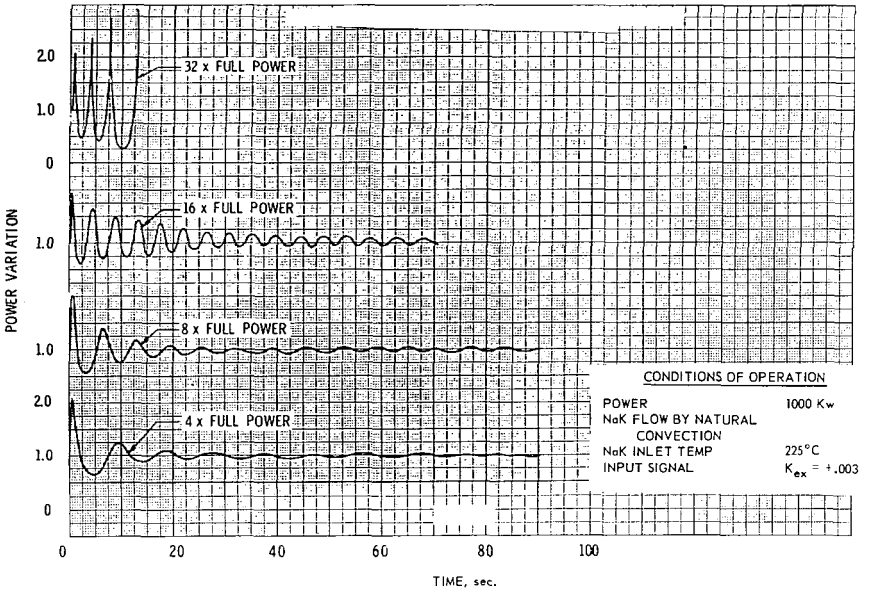

Fig. 17. Instability Produced by Increasing Feedback Gain

The high power to which it is necessary to go with the model and feedback in order to produce instability also produces temperatures above the melting points of the materials of the core. The amplitude of the oscillations produced are theoretically the same as the resonance frequency of the transfer function. There does not seem to be any well-defined resonance in the measured transfer function, shown in Figs. 26a-i. However, there would be if the transfer function were measured at the same conditions of NaK flow and reactor power. The magnitude of the step in reactivity at the high power levels has little or no influence on stability, as would be expected by analogy to a true linear system.

PRESENTATION OF MODEL PERFORMANCE IN A GENERALIZED FORM

A comparison of the responses of the reactor and model for specific combinations of operating conditions has been presented. An approximate representation of the responses of the main components of the model in parametric form and as a function of the frequency of the input signal may be of some value.

Since the change in volume of the core is considered to be the most predominant source of internal feedback ($\Delta k = c \left\{ \Delta \ell / \ell + 2\Delta R/R \right\} = 3c\, \Delta \ell / \ell$), a good approximation of the model response for any combination of operating conditions can be achieved by expressions for Δk in terms of $\Delta \ell / \ell$ only. This simplification enables the following to be determined readily by interpolation of sets of parametric presentations:

a) the open-loop sinusoidal response;
b) relative reactor stability;
c) the closed-loop sinusoidal response or "reactor transfer function"; and
d) the contributions of the various components of the model to the internal feedback due to the movement of uranium.

The frequency response of the component of the model known as the neutron kinetics equations is plotted and approximated by a function of the complex variable (s) in Fig. 18.

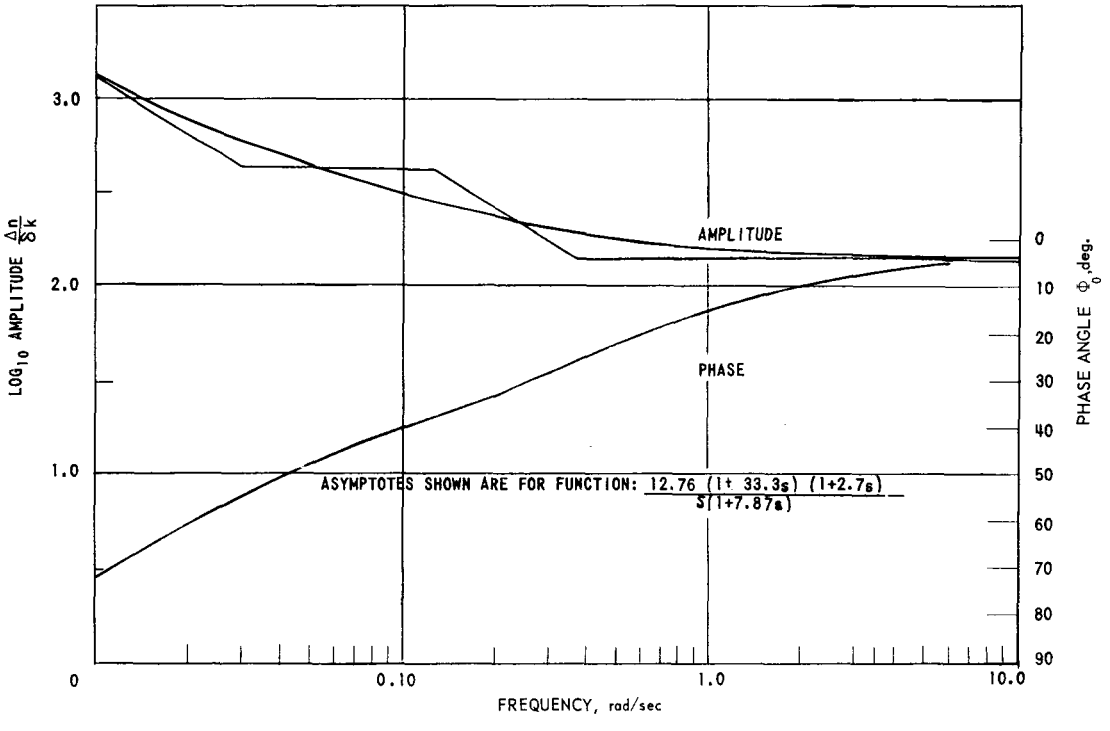

Fig. 18 Response of the Neutron Kinetic Equations

The frequency response of the combined effect of the thermal phenomena and that elastic phenomena pertaining to the interaction of the uranium rod and zirconium cladding is shown in Fig. 19.

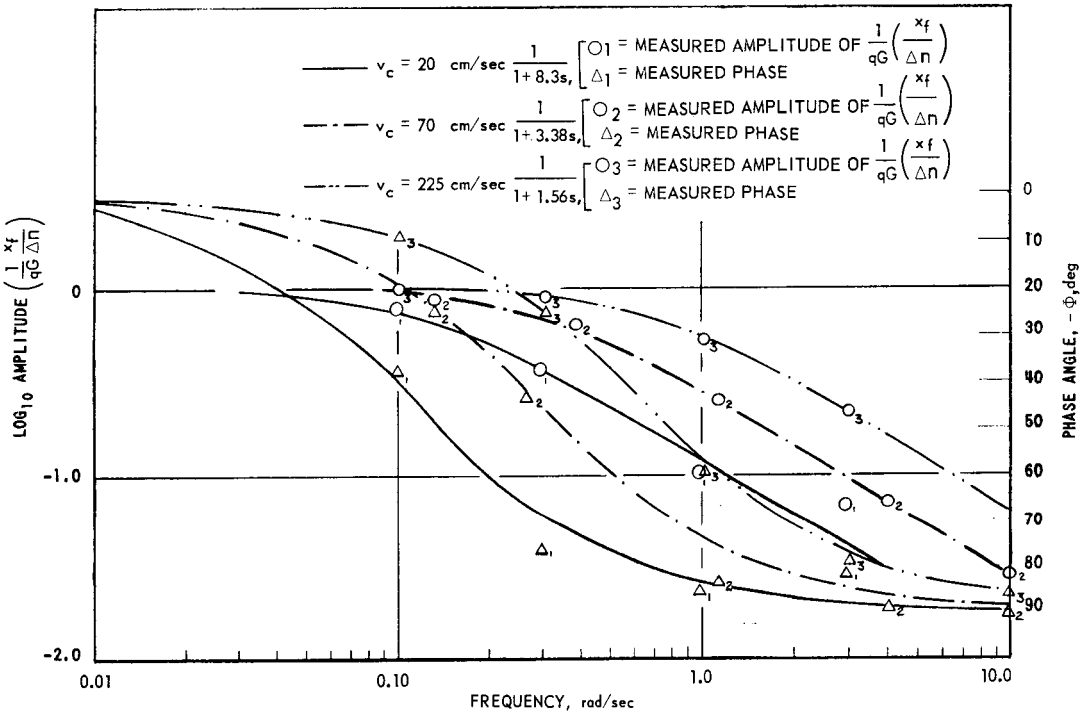

Fig. 19 The Response of the Unrestrained Thermal Phenomena

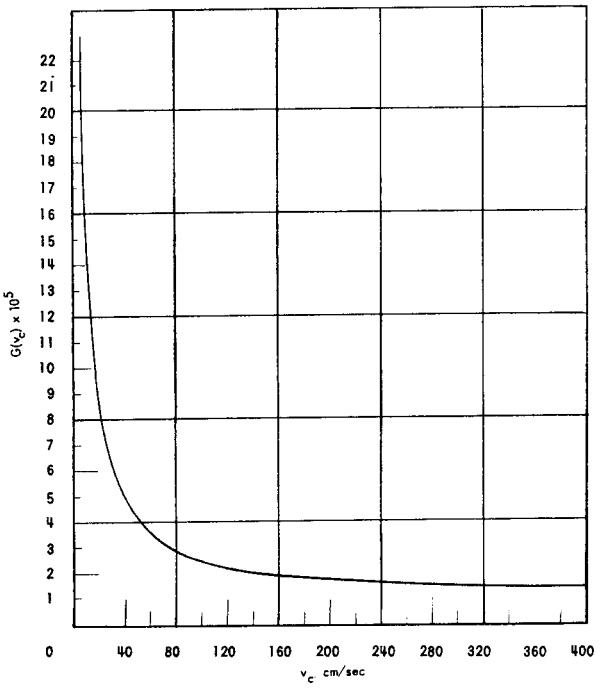

Fig. 20 $G(v_c)$ vs. v_c

The amplitude response, $x_f/\Delta n$, is the value of amplitude read from the curves of Fig. 19 multiplied by qG where G is a function of NaK velocity through the core (Fig. 20), and q is the average heat generation per cm^3 of fuel.

The response of the thermal phenomena for a step in heat generation with NaK velocity as parameter is shown in Fig. 21. The equivalent "thermal time constant" of the core is shown in Fig. 22.

The response of the fundamental of the nonlinear equations of motion, eq. (14), to the forcing function $(x_f = \Delta\ell/\ell)$ is shown in Fig. 23. This response is averaged over all rods

(hence the smooth curves rather than the equivalent curves with small discontinuities (a series of steps) which would result from the response of a single rod equivalent to the entire core).

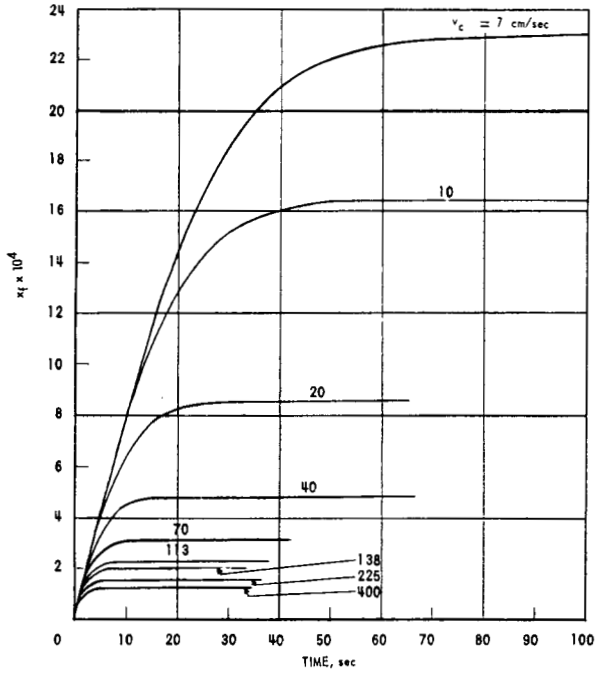

Fig. 21 Unrestrained Response of the Thermal Phenomena to Steps of q = (10 cal/cm³ sec) with v_c as Parameter

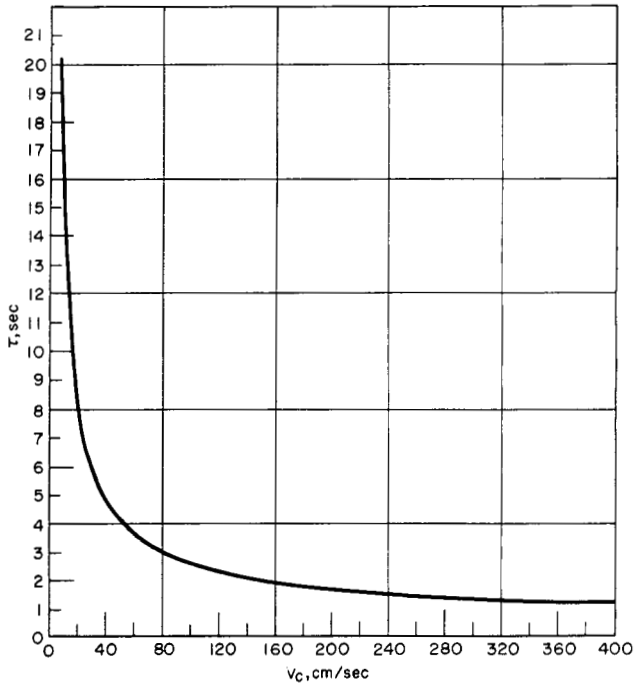

Fig. 22 Thermal Time Constant (τ vs. Coolant Velocity v_c)

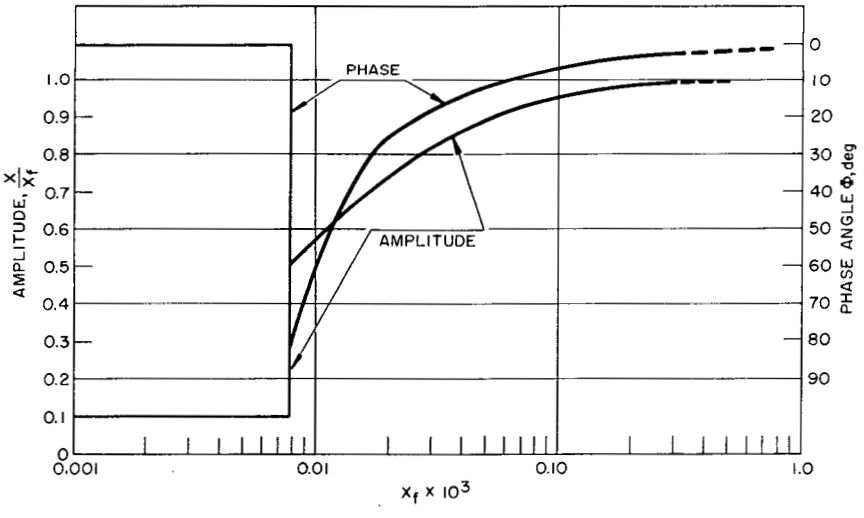

Fig. 23 Response of

$$\left[m\ddot{x} = \frac{gEA}{\ell} (x_f - x) - c\dot{x} - F/\ell - F_r/\ell \right] \text{ to } x_f$$

For an amplitude of $x_f << 7.8 \times 10^{-6}$ (corresponding to a fuel temperature of 0.5°C) the concomitant expansive force in the rods is not sufficient to overcome static friction ($\mu_0 N$), and all rods expand or contract as a unit in phase with the input. The restraint to free expansion is manifest as potential strain energy rather than as energy expended in overcoming the resistance to relative motion between rods.

The complete open-loop response is obtained by combining the contributions of the various components of the model.

$$\frac{\Delta k}{\delta k} = \frac{\Delta n}{\delta k}\left[\frac{1}{qG}\frac{x_f}{\Delta n}\right] qG \frac{x}{x_f}\frac{\Delta k}{x}$$

The term $\Delta k/x$ is a constant ($\Delta k/x = \Delta k/x_f = 1.82$). It relates a change in the volume of core to reactivity and is independent of the mechanisms causing this change. Although the constant 1.82 seems to pertain only to $x_f = \Delta \ell/\ell$ (core), it actually includes the contributions of all internal feedbacks at steady state. The constant 1.82 includes the contributions of $\Delta \ell/\ell$ (core), $\Delta \ell/\ell$ (blanket), $\Delta \rho/\rho$ (core) and $\Delta \rho/\rho$ (blanket). Since the generalized presentation of reactor response is referred to the predominant feedback due to $\Delta \ell/\ell$ (core), the multiplication by the constant 1.82 presumes that the other feedbacks are dynamically similar. Of course this is not true but, for the sake of simplicity and in view of the fact that their combined effect is relatively small compared to that of $\Delta \ell/\ell$ (core), the constant 1.82 has been used in the generalized approximation of the reactor's response.

The expression $\Delta k/\delta k$ is the describing function of the reactor; therefore the usual methods of linear analysis (i.e., Bode, Nyquist, root locus plots, etc.) may then be applied to the function $\Delta k/\delta k$ to obtain a qualitative estimate of reactor response and stability. It is important to recognize that this is based on the reactor zero-power transfer function and is valid only for values of δk less than 50% of prompt critical. When δk exceeds this value the method becomes invalid, since the presence of large δk increases the gain and phase shift of the kinetics transfer function. Since this occurs in the frequency region where an approach to instability is possible, the foregoing method may provide an appraisal of relative stability which is more optimistic than the true situation.

COMPARISON OF MODEL AND REACTOR RESPONSES

The responses of the model operating under a wide variety of conditions to a given signal are presented and compared to the measured response of the reactor operating at the same conditions.

1 - Zero-power Transfer Functions

The zero-power transfer functions were determined using the data of Hughes* and of Keepin.** The results are shown in Fig. 24.

	HUGHES DATA		KEEPIN DATA	
ω	AMPLITUDE	PHASE ANGLE	AMPLITUDE	PHASE ANGLE
0.01	1192.2	71.98	1333.9	72.44
0.02	697.0	60.97	777.2	61.88
0.04	463.9	49.28	510.7	50.70
0.06	385.1	44.07	419.1	45.48
0.08	340.0	41.24	367.5	42.46
0.1	308.8	39.26	332.7	40.28
0.2	232.9	32.55	248.9	33.15
0.4	186.0	25.01	198.2	24.53
0.6	168.4	20.46	181.5	19.62
0.8	159.5	17.40	173.2	16.66
1	154.2	15.23	168.0	14.69
2	143.2	9.71	156.0	9.72
4	137.9	5.83	149.4	5.91
6	136.3	4.35	147.3	4.24
8	135.4	3.59	146.4	3.29
10	134.8	3.13	145.9	2.68

Fig. 24 A Comparison of the Zero-power Transfer Functions Obtained from the Data of Hughes and of Keepin

2 - Responses to a Step in Reactivity

The model matches the rod-drop responses by virtue of the fact that the proper value and relationship of the effect of heat generation and NaK velocity have been achieved. The response to a step is obviously quite sensitive to NAK velocity and this sensitivity increases with an increase in heat generation.

The responses of model and reactor to a rod drop at approximately zero power are shown in Fig. 25a. The responses of model and reactor to rod drops at other conditions of operation are shown in Fig. 25b, c and d.

3 - Responses to a Sinusoidal Variation in Reactivity

The reactor values of the amplitude and phase angle of the feedback function H for NaK flows of 300 gpm and 180 gpm are plotted as a function of frequency in Figs. 10-13. Power is the parameter. The amplitude of H is power normalized to the highest power.

While the Bode plots showed the similarity in characteristics of reactor and model feedback function H, it is of interest to compare the closed-loop transfer function $\frac{n/n_0}{k_{ex}}$ (Figs. 26a-b). Since $\frac{n/n_0}{k_{ex}} = \frac{G_0}{1 + G_0 H}$, at high

---

* D. J. Hughes et al., Phys. Rev., 73, 111 (1948).

** G. R. Keepin et al., Phys. Rev., 107, 1044 (1957).

frequencies $G_0H \ll 1$ and $\frac{n/n_0}{k_{ex}}$ approaches G_0, the zero-power transfer function. At low frequencies $G_0H \gg 1$ and $\frac{n/n_0}{k_{ex}}$ approaches $1/H$.

A root locus plot of the system under these conditions indicates the presence of one pair of complex roots, which has a damping ratio of 0.8. Therefore there is no significant resonance apparent in the closed loop.

A comparison of the sinusoidal response of the reactor and model over a wide range of operating conditions is shown in Figs. 26a to 26i. The solid curves given on each are the zero-power responses for comparison.

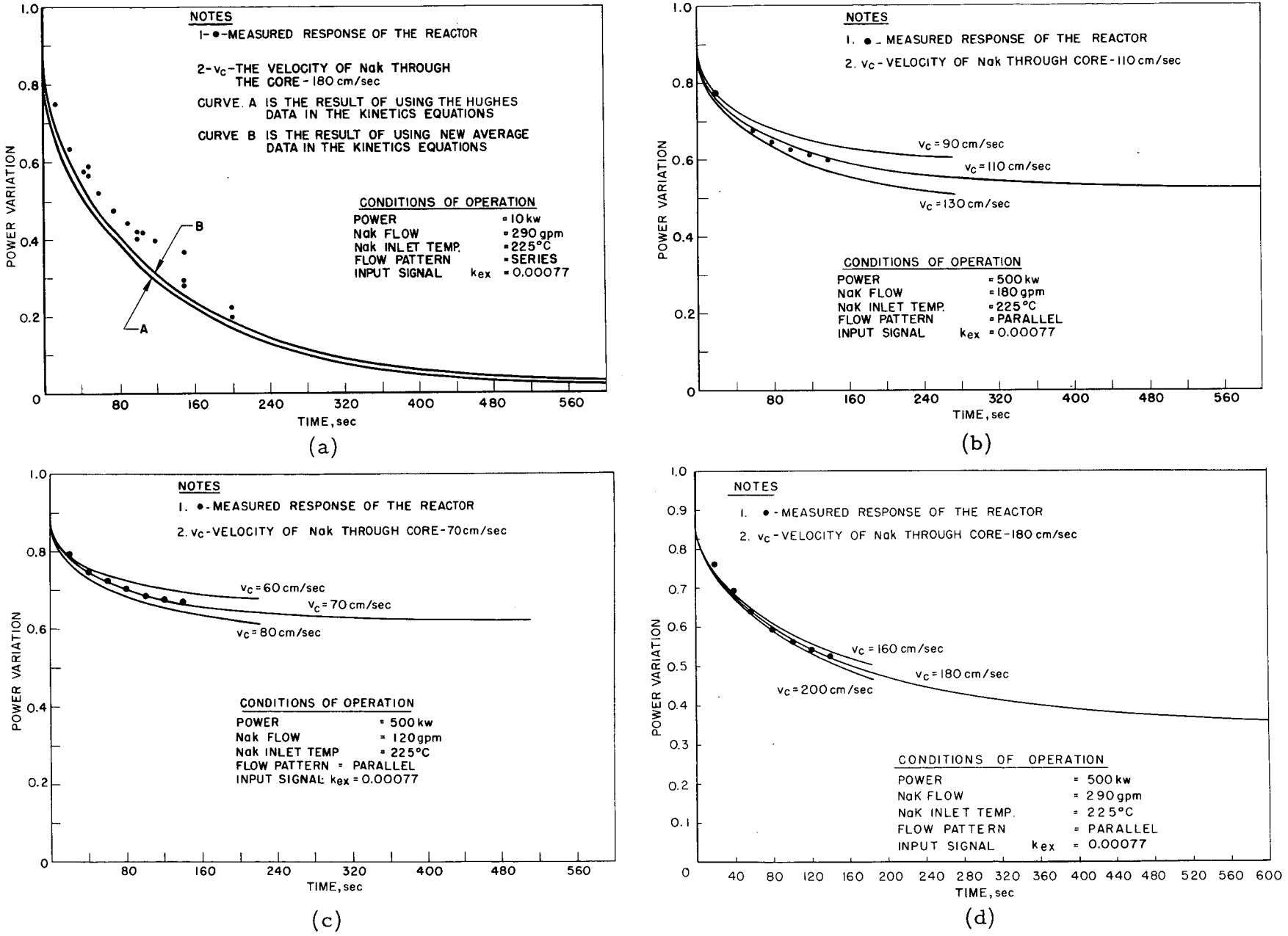

Fig. 25 Response to Step Signals; Power vs. Time

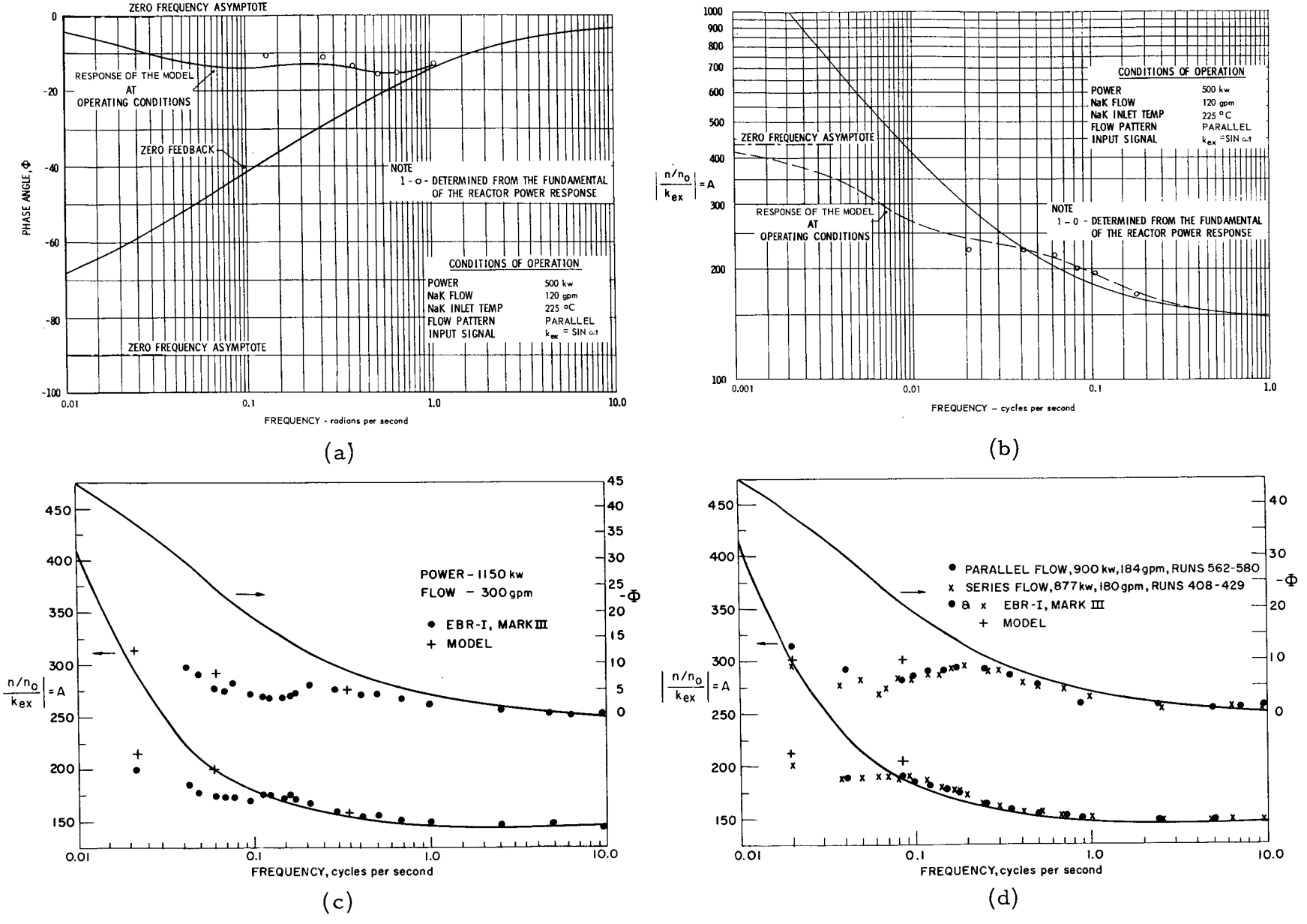

Fig. 26 Response to Sinusoidal Signals Describing Function

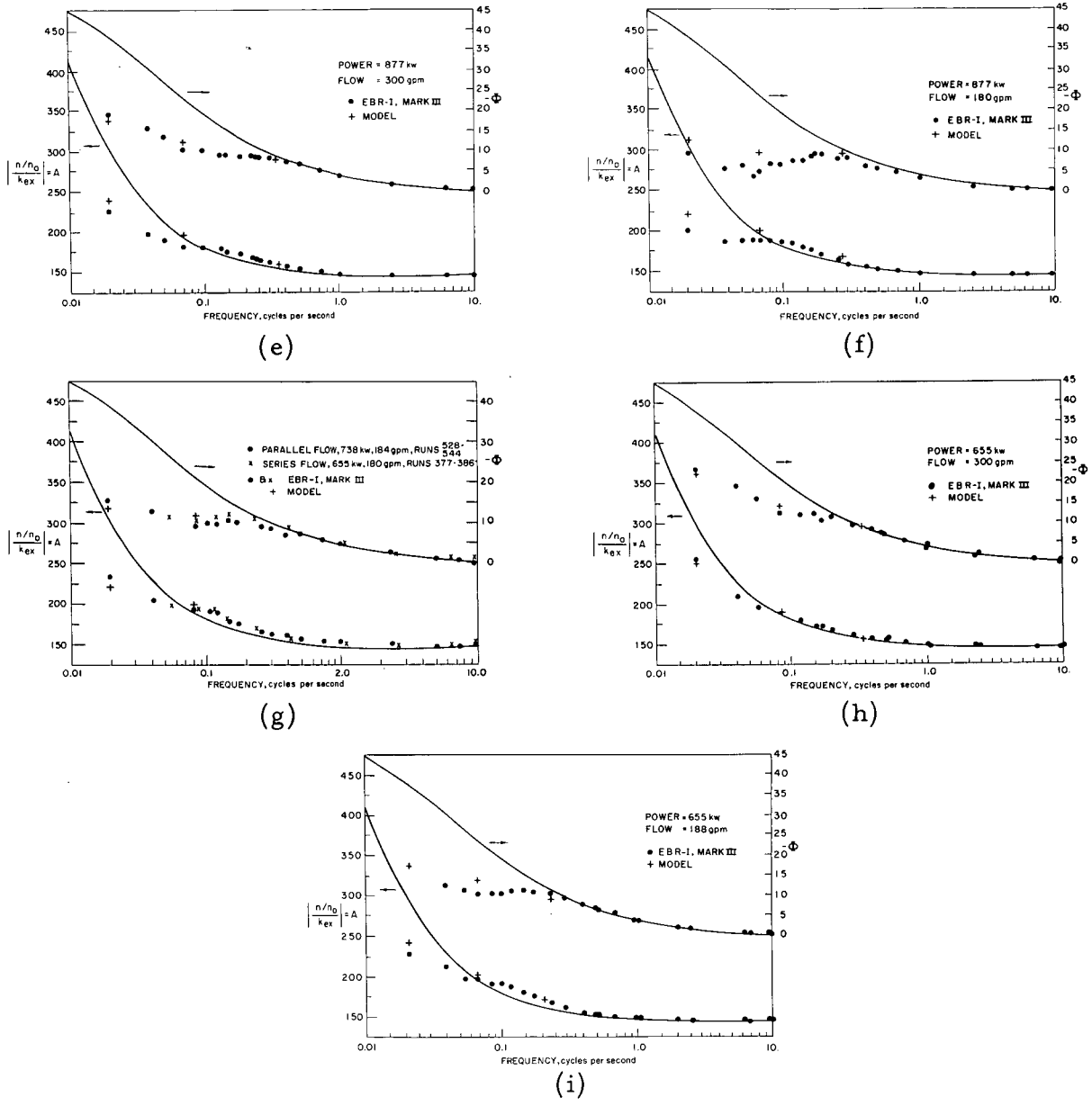

Fig. 26 Response to Sinusoidal Signals Describing Function

GENERAL DISCUSSION

The primary emphasis in the analog work thus far has been an attempt to understand the physical processes underlying the responses of Mark III. Exploration of some possible dangerous conditions of power, flow, and reactor period has been done with the present model. It can be stated, however, that, based on linear theory utilizing the describing function of the nonlinear friction restraint mechanism, the reactor would appear to be stable at indefinitely high power. The describing function of the mechanism for nonlinear motion of rods can never have more than a 90° phase lag. This lag decreases to zero as amplitude increases; hence it would appear that, if under any conditions the reactor were unstable (i.e., free resonance, or poles of the closed loop in the right half of the s plane), free oscillations would build up to a definite amplitude at which the phase lag of the friction mechanism is reduced so that the total phase lag of $\Delta k/\delta k$ is equal to 180° at the oscillation frequency at which the absolute value of $\Delta k/\delta k$ is unity.

This work has dealt only with the responses of Mark III. The ability of the Mark III Model to produce free oscillation at constant amplitude indicates that a similar process may have contributed to the dynamic behavior of Mark II, which displayed such oscillations. This has not been explored in any detail as yet. It is interesting to note, also, that subharmonics were found in Mark II sinusoidal responses. These are also found in the present model. Figure 27 shows a typical recording of the null signal (Channel 2) of the present model remaining after bucking out the fundamental component of the power response. Channel 1 is the fundamental input frequency. Channels 3 and 4 show most clearly the subharmonic frequency. The rates of drift of the average values of Channels 3 and 4 are a measure of the amplitude of fundamental remaining in the null signal. Close inspection of Channel 5, the restrained rod motion, shows that the subharmonic mechanism consists of a change from one jump per cycle to two jumps per cycle of the input. This cycle repeats regularly after many input cycles, due to small differences between size of jumps in the two directions.

The presence of subharmonics is a sure proof of the presence of a nonlinearity. Nonlinearity in itself, however, is necessary but <u>not</u> sufficient to insure subharmonic responses. While subharmonics are clearly evident in the responses of the present model, it is not clear that this requires their presence in Mark III responses. In the Mark III case, these may be averaged out by the random time of slip of the individual rods or groups of rods. It would appear, however, that the n/n_0 responses would show noise unaccounted for by nuclear processes. It is understood that some evidence of unexplained noise has been noted. A detailed spectral analysis of this noise might be of considerable value for further verification of the model.

It is believed that the weight of evidence so far presented is such that there is little doubt that the nonlinear feedback mechanism described in this paper is in fact the mechanism existing in Mark III which produces its

nonlinear characteristics. This mechanism leads to the conclusion that the reactor would be stable at any condition of operation that will not result in the melting of core materials.

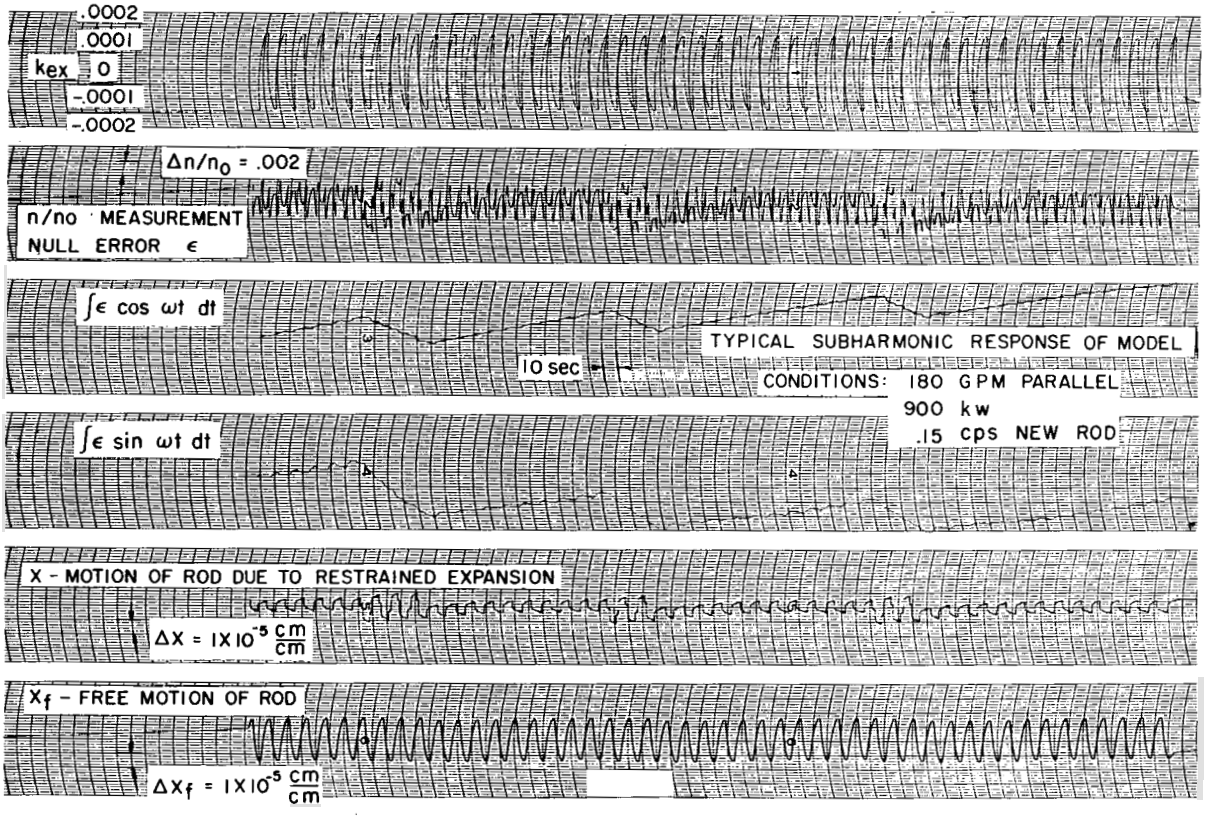

Fig. 27 Typical Recording of the Model Response

The importance of the answer to the question of stability, however, dictates investigation of the Mark-III data with the possibility in mind that, in spite of evidence to the contrary, the feedback may be due to some entirely different and as yet unknown mechanism.

Stability predictions at high power based on analysis of low-power experimental data alone, without regard to the mechanism producing the data, would be valid only if the reactor is a linear system.

It obviously is a nonlinear system, so an answer to the stability question is not possible on the basis of linear theory. It can, however, be stated with certainty that, if there are any linear feedback terms (a prompt positive term falls in this category) capable of producing instability at some power, their presence can be detected at a lower safe power level. This statement is only true if the effects of measurement error are recognized.

A Bode plot of the reactor open-loop transfer function $\Delta k/\delta k$ is shown in Fig. 28. The criterion for stability in systems of this sort, as evidenced by a root locus plot for the reactor, is that the amplitude be less than unity at frequencies for which the phase is $\geq 180°$. This criterion is absolute for linear or nonlinear terms of the feedback regardless of their source, whether it be from a prompt positive, delayed negative or any other phenomenon. The use of the plot for predicting stability at conditions of power, flow, input amplitude, etc., other than those at which the data for the plot were taken, is only valid for the linear feedback terms.

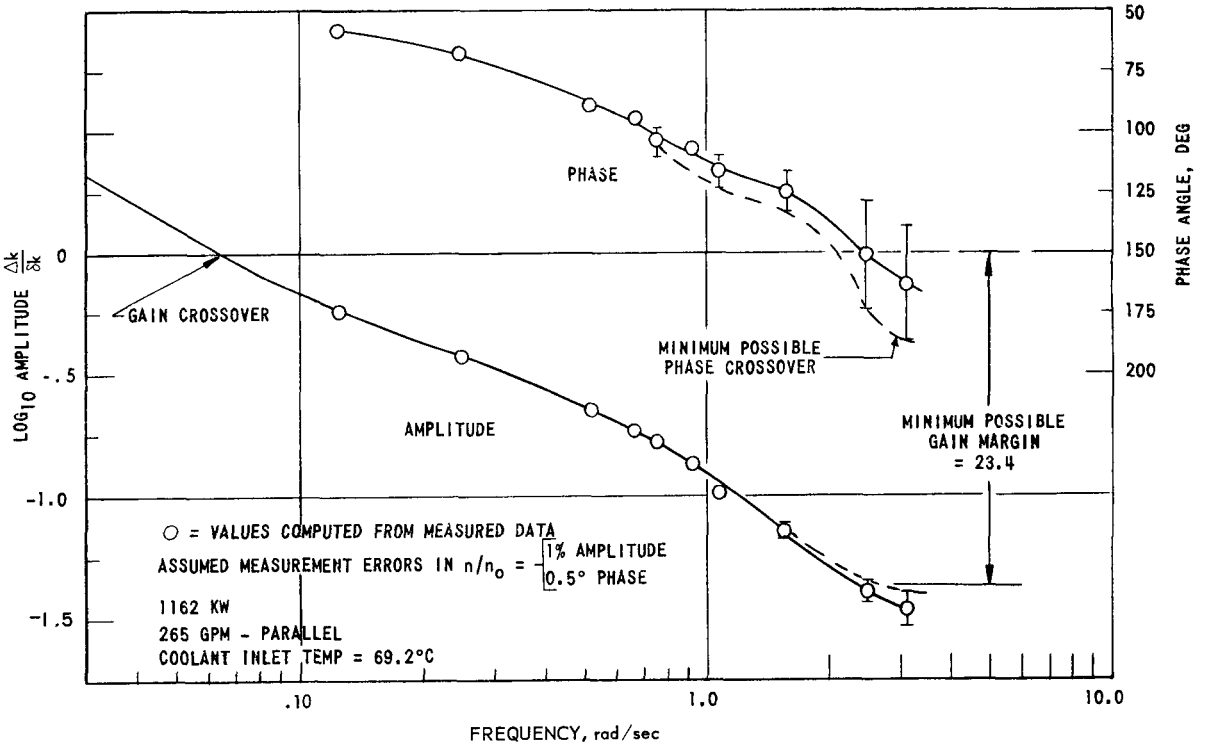

Fig. 28 Open-loop Frequency Response

From the Bode plot, a definite value can be determined for the lowest power at which instability could possibly exist as a result of any linear term in the feedback.

As may be seen in Fig. 28 the width of the error bands which result from measurement errors increase rapidly above the gain crossover frequency.* The best prediction of stability will thus be obtained from a Bode plot of data taken under conditions for which the gain crossover frequency is as near as possible to that at which the phase crossover (of 180°) occurs.

*The frequency at which the log amplitude plot crosses zero, i.e., unity amplitude ratio.

In general, to attain this, conditions are chosen which result in more lag to lower the phase crossover frequency and more gain to increase the gain crossover frequency. For this reason, natural convection flow of NaK (for maximum thermal lag) and the highest power short of melting the fuel rods were considered to be the conditions most likely to produce instability. Accordingly these conditions were used for the earlier exploratory work described in the Section titled "Exploration Work with Model."

Later frequency-response measurements on the complete model demonstrated that a closer approach to instability can be obtained using maximum flow with power at the highest level short of melting fuel at the hottest point in the core. That this is true can be verified from the data presented in the Section "Presentation of Model Performance in a Generalized Form." The reason for this is that, at frequencies near the phase crossover, the amplitude response of the thermal equations is almost independent of flow, being determined mostly by the thermal capacity of the fuel. Thus the flow which permits the highest power possible without damage to the reactor gives the closest approach to instability. Of the available Mark-III data, the set from which the Bode plot of Fig. 28 was made, represents the condition closest to instability by this criterion of proximity of gain and phase crossover frequencies. The least factor of increase of power which could result in true instability is that necessary to raise the gain crossover for the upper limit of the amplitude error band to the frequency of 2.7 rad/sec. This frequency corresponds to the phase crossover of the lower side of the phase error band. Note that a change of power from P_0 to P displaces the entire amplitude curve vertically by log (P/P_0). Letting P_0 be the power at which the data were taken, and P be the least possible power for instability indicated by this data, then P/P_0 is the minimum possible gain margin. From Fig. 28 it may be seen that

$$\log P/P_0 = 1.37$$

or

$$P = (23.4)\ P_0 \quad ,$$

so that

$$P = 1.162 \text{ Mw} \times (23.4) = 27.2 \text{ Mw}.$$

From measurements on the complete analog model, which assumes uniform flow throughout the core, it has been found that at coolant inlet temperature of 60°C and flow of 300 gpm it should be possible to reach a power of 9.1 megawatts before the melting point of uranium is reached at the hottest point in the core. Thus it appears that, by the most pessimistic possible interpretation of presently known Mark-III data, it is not possible to attain instability.

The best answer to the question of ultimate stability of a nonlinear system will always be obtained by an analog computer solution of the equations of the physically plausible mechanism which best explains all responses observed in the system under known safe conditions. For EBR-I, Mark III it is believed that this is the feedback mechanism described in this paper. The answer to the stability question provided by this mechanism can be obtained from the curves given in Figs. 18-23.

In order to have true instability at any power it is necessary that the open loop function $\Delta k/\delta k$ reach 180° phase shift at some real frequency. The data presented actually show no condition in which the total phase is greater than 178°, indicating that the reactor can never be unstable at any power. Approximations made in writing the thermal equations of the model are such that enough additional phase lag to produce a phase crossover at a real frequency is quite possible.

If this were the case and the equation error were as large as 9.5°, the curves would predict the same minimum power (27.2 Mw) for instability as was predicted by the linear analysis before. The curves predict that the gain crossover, hence the frequency of natural oscillation, occurs at 2.5 rad/sec. If flow could be increased enough to permit exceeding this power without melting fuel, linear analysis would predict oscillations of indefinitely increasing amplitude. The response of the model, however, would only increase to a small amplitude at which the phase of x/x_f (Fig. 23) is reduced so that the total phase is exactly 180°. For example, assume that power were set at 30 Mw, and the total phase of $\Delta k/\delta k$ were 16.5° more than that given by the model equations. This would produce a total phase 8.0° beyond 180° at the gain crossover frequency of 3.0 rad/sec. The amplitude of the oscillations resulting would then build up until the phase of x/x_f were reduced from its maximum of 82° by the amount 8.0°.

Figure 23 shows that this occurs at x_f amplitude of about 8.5×10^{-6}. This corresponds to a fuel temperature oscillation of about 0.5°C about the operating temperature, which is inconsequential.

The most pessimistic possible interpretation of present data predicts 27.2 Mw as the minimum value for instability. The most probably correct interpretation predicts a minimum equal to or greater than this, but that the oscillations produced would be of no consequence. Thus we may say with conviction that presently known responses in EBR-I, Mark III indicate that there is no possibility of damage ever resulting from self-excited oscillations building up spontaneously from a condition of equilibrium at any attainable power.

The situation regarding responses to inputs resulting in Δk above 50 cents is considerably less certain. As mentioned before, the Bode plot of the neutron kinetics section given in Fig. 18 is only valid for δk less

than this value. The changes in the plot for δk above 50 cents are such that the reactor rapidly approaches instability even at normal power as δk approaches prompt critical. Preliminary experiments on the model mentioned in the Section, "Exploration Work with Model" indicate that even a prompt critical step input would not cause melting temperatures. Much more exhaustive analog studies are required, however, before any such experiment on the reactor could be considered safe.

CONCLUSIONS

1. The feedback of EBR-I, Mark III is such that this reactor has dynamic characteristics which cause it to be stable well beyond its operating range. The large negative feedback is considered to be due to the condition that the spaced fuel rods cause the core to expand as a solid cylinder.

   If the spacers are removed from the core section, the negative feedback should be less; hence there will be a smaller power coefficient and reduced inherent stability. The feedback should also show less phase shift and less hysteresis at low fuel temperatures. At high fuel temperatures it is possible that elastic buckling of the fuel rods could occur. This would cause a positive feedback in addition to the diminished negative, and the reactor could become dangerously unstable.

2. EBR-I, Mark III is a nonlinear system and accordingly should be represented by a nonlinear model. Linear analysis using the root locus method indicates a greater margin of safety than does the nonlinear model.

3. A large delayed negative coefficient can cause instability, but an unrealistically high power.

4. The reactor closed-loop transfer function increases with decreasing fuel temperature.

5. A prompt positive coefficient capable of producing instability can exist and not be detected at normal operating conditions by qualitative inspection of response data. However, it can always be detected by a careful analysis of the operating data and of the effect of possible errors in the measurement of this data.

6. Mathematical models of nuclear reactors and an electronic analog computer provide a safe and rapid means of investigating the dynamic characteristics of reactors prior to operation and are of great assistance in the attempt to reconcile the discrepancies between measured results and theoretical predictions.

7. It is possible to construct an analog model of a reactor from analysis that has sufficient dynamic similarity to predict the performance of the reactor to the extent that there will be no unfortunate surprises when the reactor goes into operation.

APPENDIX A

Dimensions and Physical Data for EBR-I Core

The dimensions and physical data pertaining to the analysis of the Mark-III EBR-I core are listed below.

U-Zr Rods

19 hexagons: 7 in the core and 12 in the blanket
36 U rods per hex. 1 steel wedging rod.

Length of lower blanket section = 9.04875 cm
Length of core section = 20.9550 cm
Length of upper blanket section = 19.6850 cm

Dia. of U rod = 0.92456 cm
Dia. of Zr cyl. = 1.02616 cm

Sectional area of one U rod = 0.671395 cm^2
Sectional area of one Zr cyl. = 0.155667 cm^2
% of area which is Zr = 18.8

Surface of Zr per rod which is available for heat transfer = 3.224 cm^2/cm

Area for NaK Flow

Outside area of hexagon = 46.1826 cm^2
Inside area of hexagon = 43.4942 cm^2
Area of U + Zr per rod = 0.82708 cm^2
Area of Zr spacer wire = 0.01072 cm^2
Area for NaK flow per hex. = 11.7017 cm^2
Area for NaK flow (parallel flow in core and blanket) = 222.3359 cm^2
Area for NaK flow (series) { downward in blanket = 140.3955 cm^2; upward in core = 81.9404 cm^2

Area for NaK Flow through the Circular Channels in the Shell

Number of channels = 12
Length of channels = 50 cm
Area per hole = 5.7008 cm^2
Total flow area = 68.4096 cm^2

Inside surface of Zr hex can = 24.6 cm^2 per cm of length
Outside surface of Zr hex can = 25.2 cm^2 per cm of length.

Physical Properties of Materials at 300°C

	U^{235}	Zr	304 S. S.	NaK	References
Density, ρ, gm/cm^3	19.05	6.55	7.93	0.800	1,2
Specific heat, c_p, cal/gm°C	0.0426	0.081	0.107	0.21	1,5,2
Conductivity, k, cal/cm sec°C	0.078	0.037	0.051	0.062	1,5

α and E as Functions of Temperature[1,3,4]

$$\alpha_u = 15.56 \times 10^{-6} - 5.15 \times 10^{-9}\, T + 2.09 \times 10^{-11}\, T^2 \text{ cm/cm°C}$$

$$\alpha_z = 4.54 \times 10^{-6} + 4.24 \times 10^{-9}\, T - 2.77 \times 10^{-2}\, T^2 \text{ cm/cm°C}$$

$$E_u = 19.7 \times 10^{8} - 9.81 \times 10^{5}\, T \text{ gm/cm}^2$$

$$E_z = 9.90 \times 10^{8} - 8.0 \times 10^{5}\, T \text{ gm/cm}^2$$

1. Basic Materials for the Atomic Energy Industry, 2nd Ed., Natl. Lead Co., 111 Broadway, New York 6, N.Y.

2. TID-5277, Liquid Metals Handbook, Sodium-NaK Supplement, AEC (July 1, 1955).

3. Journal of Metals, 8, 1282 (1956).

4. R. B. Russell, The Coefficients of Thermal Expansion for Zirconium, MIT-1073 (Oct. 1951).

5. Zirconium and Its Alloys, in the Reactor Handbook, General Properties of Materials, AECD-3647, Vol. 3, p. 471, Sect. 1 (1955).

APPENDIX B

Numerical Values of Constants in Eq. (1)

Physical Constants:

$g = 980 \text{ cm/sec}^2$

$E = 16 \times 10^8 \text{ gm/cm}^2$

$A = 168.8 \text{ cm}^2$

$\ell = 21 \text{ cm}$

Assumed Values:

$\mu_0 = 1.00$

$\zeta = 1.00$

$\epsilon = 20 \times 10^{-4} \text{ cm/sec}$

$\omega_0 = 2\pi \times 4000 \text{ rad/sec}$

Determined by Computer Experimentation to Fit Mark-III Data at NaK inlet temperature of 225°C:

$\Delta x_0 = 0.12 \times 10^{-4}$

$\delta = 0.70$

$C_f = 0$

Calculated from above:

$k = gEA/\ell = 1.26 \times 10^{13} \text{ dynes/cm}$

$m = k/\omega_0^2 = 19.7 \text{ kg}$ (total mass of U in core = 68 kgm)

$c = 2k\zeta/\omega_0 = 1.00 \times 10^9 \text{ dynes/cm/sec}$ (critical damping)

$$\alpha = \frac{1}{1 - \delta/f(\zeta)} = 3.3$$

$F_r = \mu_0 N = \ell k \Delta x_0$

$F = F_r/\alpha$

$P = 94 \text{ psi}$

P is an equivalent hydrostatic pressure in the reactor tank determined by the normal force per unit area required at the core boundary.

APPENDIX C

Glossary of Terms Common in Reactor Kinetics

Autocorrelation function (T) = $\overline{f(t)\, f(t+T)}$

The average value of a function multiplied by the same function after it has been offset by a given time, the average value being expressed as a function of the offset time.

Block Diagram

A diagram, which identifies components in blocks and shown signal paths between blocks, used to describe a system. A block should include a logical portion of the system.

Convolution

The process of finding the total response of a system as the sum of the responses of individual impulses.

Describing Function

The ratio of the fundamental component of the output to the amplitude of the input for a nonlinear element.

Error

The difference between the input and the output signal, or the difference between the actual output and the desired output.

Internal Feedback

That phenomenon inherent in the design of a specific reactor which makes the input signal a function of the output.

Linear System

A system whose characteristics are independent of the amplitude of the signal or of time, i.e. described by a set of linear differential equations with constant coefficients.

Multicoupled System

A system in which the signal paths in the block diagram are intercoupled to the extent that direct simplification is not possible.

Multiloop System

A system whose block diagram has several loops. Simplification can be achieved by successively replacing a loop with a single block.

Noise

An unwanted or false input signal.

Nonlinearity

The term "nonlinearity" pertains to any phenomenon which is described by nonlinear differential equations.

Pole

A value of s which causes a given function, usually G(s), to become infinite. A pole is usually denoted by a cross on root-locus plots.

Response (Frequency)

The term frequency response of a system refers to the change in magnitude and the shift in angle of sinusoidal signals of various frequencies in being transmitted throughout the system. The characteristics may be calculated or measured and provide a means of studying the stability of the system.

Response (Transient)

The natural response of a system due to any disturbance, such as a sudden change in the input signal.

Root Locus

For a system whose characteristic equation is $KG(s) + 1 = 0$, the root locus is a plot in the s plane of the values of s which make G(s) a negative real number. A point along the locus is a root if the gain K is selected such that $KG(s) = -1$.

Root Locus Method

A transient response can be expressed as the sum of terms of the form e^{st}. The values of s are roots of the characteristic equation of the system. The root locus method determines these roots graphically using simplifications suggested by the form of the equation for a control system.

Time Constant

The time constant λ is defined as the time in seconds for the feedback due to the change in a physical property, $\Delta J/J$, to increase to $(1 - \frac{1}{e})$ of its full value.

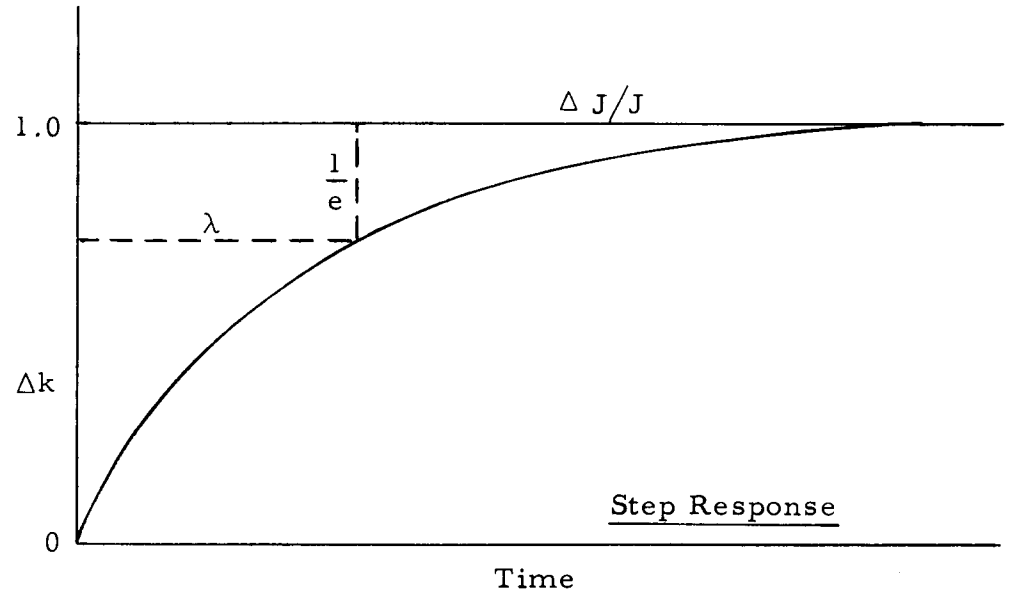

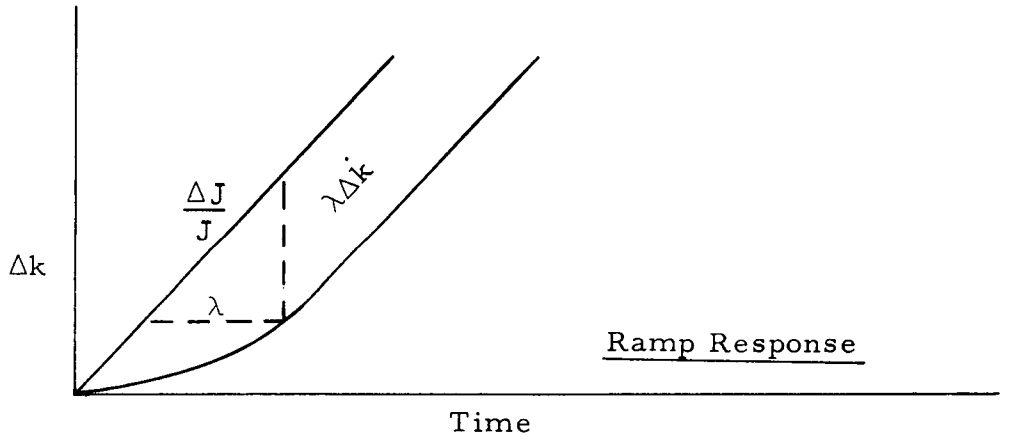

$$\lambda \Delta \dot{k} = \frac{\Delta J}{J} - \Delta k$$

$$\Delta k\,(s)\,(1 + \lambda S) = \left(\frac{\Delta J}{J}\right)$$

$$\Delta k(s) = \frac{1}{(1 + \lambda S)} \left(\frac{\Delta J}{J}\right)$$

Time Lag or Transport Delay

Frequently in the study of the dynamics of reactors the expression $f(t - \tau)$ occurs and it is difficult to simulate on an analog without special and expensive equipment.

The following scheme is considered to give a good approximation with a fairly simple circuit. It is based upon the mathematical approximation to the Laplacian shift operator $e^{-s\tau}$.

The Laplace transform of $f(t - \tau)$ is

$$\int_0^\infty f(t)\, e^{-st}\, dt = F(s)$$

$$\int_\tau^\infty f(t - \tau)\, e^{-s(t - \tau)}\, dt = F(s) \quad .$$

Multiplying both sides by $e^{-s\tau}$

$$\int_0^\infty f(t - \tau)\, e^{-st}\, dt = e^{-s\tau}\, F(s) \quad .$$

The problem of generating a function $f(t - \tau)$ can therefore be reduced to that of generating the function $e^{-s\tau}$. The Taylor series expansion converge too slowly for practical purposes. Too much analog equipment is tied up in this circuitry. A practical analog circuit for τ up to 60 sec results from an approximation for e^x due to Padé.* The Padé approximation is:

$$e^x = \lim_{(u+v)\to\infty} \frac{F_{u,v}(x)}{G_{u,v}(x)}$$

$$F_{u,v}(x) = 1 + \frac{vx}{(u+v)\,1!} + \frac{v(v-1)x^2}{(u+v)(u+v-1)\,2!} + \cdots + \frac{v(v-1)\cdots 2\cdot 1 x^v}{(u+v)(u+v-1)\cdots(u+1)v!}$$

$$G_{u,v}(x) = 1 - \frac{ux}{(v+u)1!} + \frac{u(u-1)x^2}{(v+u)(v+u-1)2!} + \cdots + \frac{u(u-1)\cdots 2\cdot 1 x^u}{(v+u)(v+u-1)\cdots(v+1)u!}$$

The convergence for this series expansion is quite rapid and a value for u and v of 2 gives good accuracy for the time lags and frequencies considered.

---

*O. Perron, Die Lehre von der Kettenbruchen, Chelsea Publ. Co., New York (1950), p.424.

For u = v = 2

$$e^{-s\tau} \cong \frac{s^2\tau^2 - 6\,s\tau + 12}{s^2\tau^2 + 6\,s\tau + 12} \tag{1}$$

In terms of the original problem generating f (t - τ) when f (t) is known the equation for the second order Pade approximation can be expressed in transfer-function notation as

$$\frac{f\,(t-\tau)}{f\,(t)} \cong \frac{p^2\tau^2 - 6\,p\tau + 12}{p^2\tau^2 + 6\,p\tau + 12} \tag{2}$$

The justification for writing this expression (eq. 2) is

$$\mathcal{L} f\,(t-\tau) = F\,(s)\, e^{-s\tau} \tag{3}$$

$$\mathcal{L} f\,(t-\tau) = \mathcal{L} f\,(t)\, e^{-s\tau} \tag{4}$$

Substituting eq. 1 into eq. 4

$$\frac{\mathcal{L} f\,(t-\tau)}{\mathcal{L} f\,(t)} \cong \frac{s^2\tau^2 - 6\,s\tau + 12}{s^2\tau^2 + 6\,s\tau + 12}$$

$$(s^2\tau^2 - 6\,s\tau + 12)\,\mathcal{L} f(t-\tau) = (s^2\tau^2 - 6s\tau + 12)\,\mathcal{L} f t \tag{5}$$

The inverse transform of this is

$$(p^2\tau^2 + 6\,p\tau + 12)\, f\,(t-\tau)\; (p^2\tau^2 - 6\,p\tau + 12)\, f\,(t)\,. \tag{6}$$

Equation 5 and eq. 6 are identical as the Laplacian operator and the differential operator may be used interchangeably provided the initial conditions in a system are identically zero.

Solving the equation 6 for f (t - τ) and collecting terms according to powers of p

$$f\,(t-\tau) = f\,(t) - \left[\frac{6}{\tau} f\,(t) + \frac{6}{\tau} f\,(t-\tau)\right] \frac{1}{p} + \left[\frac{12}{\tau^2} f\,(t) - \frac{12}{\tau^2} f\,(t-\tau)\right] \frac{1}{p^2}$$

The analog diagram and a comparison of the Pade approximation with the ideal are shown on Fig. 29.

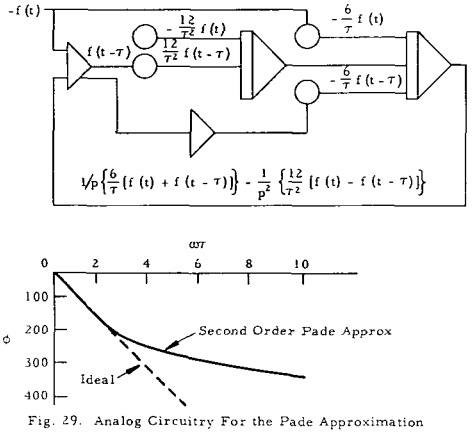

Fig. 29. Analog Circuitry For the Pade Approximation

Transform

The transfer function needed to create a given signal from a unit impulse. This definition includes initial conditions, just as does the formal definition by the Laplace transform initial.

Transfer Function

A transfer function is obtained by writing the differential equation relating output to input, replacing the operation d/dt by the complex number s, and solving for the ratio of output to input.

$$\text{Transfer Function} = \frac{\mathcal{L}\,[\text{output}]}{\mathcal{L}\,[\text{input}]}$$

Unit Impulse

A large signal acting for a short time so that the integral of the signal with respect to time is unity.

Unit Step

A sudden change in a signal of unit magnitude.

Zero

A value of s which makes a given function, usually G(s), zero. On root-locus plots, a zero is denoted by a small circle o.

BIBLIOGRAPHY

1. Ahrendt, W. R., Servomechanism Practice, McGraw-Hill Book Company, Inc., New York (1954).

2. Andronow, A. A., and C. E. Chaikin, Theory of Oscillations, English translation by S. Lefschetz, Princeton University Press, Princeton, N. J. (1949).

3. Bode, H. W., Network Analysis and Feedback Amplifier Design, D. Van Nostrand Company, Inc., Princeton, N. J. (1945).

4. Bronwell, A., Advanced Mathematics in Physics and Engineering, McGraw-Hill Book Company, Inc., New York (1953).

5. Brown, G. S., and D. P. Campbell, Principles of Servomechanisms, John Wiley & Sons, Inc., New York (1948).

6. Brune, O., Synthesis of a Finite Two-terminal Network Whose Driving-point Impedance Is a Prescribed Function of Frequency, J. Math. Phys., (October 1931).

7. Chesnut, H., and R. W. Mayer, Servomechanisms and Regulating Systems Design, John Wiley & Sons, Inc., New York (1951).

8. Churchill, R. V., Introduction to Complex Variables and Applications, McGraw-Hill Book Company, Inc., New York (1948).

9. Churchill, R. V., Modern Operational Mathematics in Engineering, McGraw-Hill Book Company, Inc., New York (1944).

10. Coblenz, A., and H. L. Owens, Transistors: Theory and Application, McGraw-Hill Book Company, Inc., New York (1955).

11. Darlington, S., The Potential Analog Method of Network Synthesis, Bell System Tech. J., 30, pp. 315-365 (April 1951).

12. Davis, S. A., Mechanical Components for Automatic Control, Product Eng. (September 1954).

13. Davis, S. A., Rotating Components for Automatic Control, Product Eng. (November 1953).

14. Evans, W. R., Control-System Dynamics, McGraw-Hill Book Company, Inc., New York (1954).

15. Evans, W. R., Control System Synthesis by Root Locus Method, Trans. AIEE, 69, pp. 66-69 (1950).

16. Evans, W. R., Graphical Analysis of Control Systems, Trans. AIEE, 67, pp. 547-551 (1948).

17. Foster, R. M., A Reactance Theorem, Bell System Tech. J. (April 1924).

18. Gardner, M. F., and J. L. Barnes, Transients in Linear Systems, John Wiley & Sons, Inc., New York (1948).

19. Gibson, J. E., A Dynamic Root-locus Plotter, Control Eng., 3 (2) (February 1956).

20. Goldman, S., Frequency Analysis, Modulation, and Noise, McGraw-Hill Book Company, Inc., New York (1948).

21. Greif, H. D., Describing Function Method of Servo-Mechanism Analysis Applied to Most Commonly Encountered Nonlinearities, Trans. AIEE, part 2, 72, pp. 243-248 (1953).

22. Guillemin, E. A., Communication Networks, John Wiley & Sons, Inc., New York (1942), Vol. 2.

23. Guillemin, E. A., Introductory Circuit Theory, John Wiley & Sons, Inc., New York (1953).

24. Guillemin, E. A., A Note on the Ladder Development of RC Networks, Proc. IRE, 40(4) pp. 482-485 (1952).

25. Guillemin, E. A., A Summary of Modern Methods of Network Synthesis, Advances in Electronics, Vol. 3, Academic Press Inc., New York (1951).

26. Houdyshell, H. H., Precision Potentiometer Life and Reliability, Presented at the Electronics Components Conference, (May 1955).

27. Hurwitz, A., Uber die Bedingungen, unter welchen eine Gleichung mit negativen reelen teilen besitzt (The conditions under which an equation has only roots with negative real parts), Math. Ann., 46, pp. 273-284 (1895).

28. IRE Standards on Terminology for Feedback Control Systems, Proc. IRE, 44 (January 1956).

29. James, H. M., N. B. Nichols, and R. S. Phillips, Theory of Servomechanisms, McGraw-Hill Book Company, Inc., New York (1947).

30. Klass, P. J., Inertial Guidance, Special Report, Aviation Week, (1956).

31. Kochenburger, R. J., A Frequency Response Method for Analyzing and Synthesizing Contactor Servomechanisms, Trans. AIEE, 69, pp. 270-284 (1950).

32. Kryloff, N., and N. Bogoliuboff, Introduction to Nonlinear Mechanics, Princeton University Press, Princeton, N. J. (1943).

33. Lienard, A., Etude des oscillations entretenues (Study of Self-excited Oscillations), Rev. gen. elec., Vol. 23, (1928).

34. Locke, A. S., Guidance, D. Van Nostrand Company, Inc., Princeton, N. J. (1955).

35. MacColl, L. A., Fundamental Theory of Servomechanisms, D. Van Nostrand Company, Inc., Princeton, N. J. (1945).

36. McLachlan, N. W., Nonlinear Differential Equations, Oxford University Press, New York (1950).

37. Minorsky, N., Introduction to Nonlinear Mechanics, J. W. Edwards, Publisher, Inc., Ann Arbor, Mich. (1947).

38. Nixon, F. E., Principles of Automatic Controls, Prentice-Hall, Inc., Englewood Cliffs, New Jersey (1953).

39. Pipes, L. A., Operational Methods in Nonlinear Mechanics, University of California Press, Los Angeles, Calif. (1951).

40. Reddick, H. W., and F. H. Miller, Advanced Mathematics for Engineers, John Wiley & Sons, Inc., New York (1947).

41. Routh, E. J., Dynamics of a System of Rigid Bodies, 3d ed., Macmillan Co., Ltd., London (1877).

42. Ryder, R. M., and R. J. Kirchner, Some Circuit Aspects of the Transistor, Bell System Tech. J., 28(3) (July 1949).

43. Savant, C. J., A Nonlinear Computer for the Solution of Servomechanism Problems, Ph.D. Thesis, California Institute of Technology, (1953).

44. Savant, C. J., How to Design Notch Networks, in Electronics Engineering Manual, Vol. 7, pp. 242-245, McGraw-Hill Book Company, Inc., New York (1953).

45. Savant, C. J., and C. A. Savant, Notch Network Design, Electronics, 28(9) p. 172 (1955).

46. Schmidt, H. A., The Precision Potentiometer as a Voltage Divider, Product Eng., Annual Handbook of Product Design for 1954, McGraw-Hill Book Company, Inc., New York.

47. Schultz, M. A., Control of Nuclear Reactors and Power Plants, McGraw-Hill Book Company, Inc., New York (1955).

48. Seely, S., Electron-tube Circuits, McGraw-Hill Book Company, Inc., New York (1950).

49. Shea, R. F., Transistor Circuits, John Wiley & Sons, Inc., New York (1953).

50. Slater, J. M., and D. B. Duncan, Inertial Navigation, Aeronaut. Eng. Rev., (January 1956).

51. Soroka, W. W., Analog Methods in Computation and Simulation, McGraw-Hill Book Company, Inc., New York (1954).

52. Stoker, J. M., Nonlinear Vibrations in Mechanical and Electrical Systems, Interscience Publishers, Inc., New York (1950).

53. Sutherland, Robert L., Engineering Systems Analysis Addison-Wesley Publishing Company, Inc., Reading, Mass. (1958).

54. Thaler, G. J., and R. G. Brown, Servomechanisms Analysis, McGraw-Hill Book Company, Inc., New York (1953).

55. Thomason, J. G., Linear Feedback Analysis, McGraw-Hill Book Company, Inc., New York (1955).

56. Truxal, J. G., Automatic Feedback Control System Synthesis, McGraw-Hill Book Company, Inc., New York (1955).

57. Tsien, H. S., Engineering Cybernetics, McGraw-Hill Book Company, Inc., New York (1954).

58. Van Valkenburg, M. E., Network Analysis, Prentice-Hall, Inc., Englewood Cliffs, N. J. (1955).

59. Von Karmon, T., and M. A. Biot, Mathematical Methods in Engineering, McGraw-Hill Book Company, Inc., New York (1940).

60. Westinghouse Tech. Data Bull. 52-600, October, 1954.

61. Wiener, Norbert, Cybernetics, John Wiley & Sons, Inc., New York (1948).